Natural strain variation reveals diverse biofilm regulation in squid-colonizing *Vibrio fischeri*

Ella R. Rotman[1,†], Katherine M. Bultman[2,†], John F. Brooks II[1,4], Mattias C. Gyllborg[1], Hector L. Burgos[2], Michael S. Wollenberg[3], Mark J. Mandel[1,2,*]

[1] Department of Microbiology-Immunology, Northwestern University Feinberg School of Medicine, Chicago, IL USA

[2] Department of Medical Microbiology and Immunology, University of Wisconsin-Madison, Madison, WI USA

[3] Department of Biology, Kalamazoo College, Kalamazoo, MI USA

[4] Current address: Department of Immunology, The University of Texas Southwestern Medical Center, Dallas, TX USA

[†] Authors contributed equally

Short title: *Vibrio fischeri* biofilm regulatory evolution

Keywords: Biofilm, phosphorelay, RscS, BinK, Vibrio fischeri, Aliivibrio fischeri

* Correspondence to:

Mark J. Mandel
University of Wisconsin-Madison
Department of Medical Microbiology and Immunology
1550 Linden Drive
Madison, WI 53706
Phone: (608) 261-1170
Fax: (608) 262-8418
Email: mmandel@wisc.edu

ABSTRACT

The mutualistic symbiont *Vibrio fischeri* builds a symbiotic biofilm during colonization of squid hosts. Regulation of the exopolysaccharide component, termed Syp, has been examined in strain ES114, where production is controlled by a phosphorelay that includes the inner membrane hybrid histidine kinase RscS. Most strains that lack RscS or encode divergent RscS proteins cannot colonize a squid host unless RscS from a squid symbiont is heterologously expressed. In this study, we examine *V. fischeri* isolates worldwide to understand the landscape of biofilm regulation during beneficial colonization. We provide a detailed study of three distinct evolutionary groups of *V. fischeri* and find that while the RscS-Syp biofilm pathway is required in one of the groups, two other groups of squid symbionts require Syp independent of RscS. Mediterranean squid symbionts, including *V. fischeri* SR5, colonize without an RscS homolog encoded in their genome. Additionally, Group A *V. fischeri* strains, which form a tightly-related clade of Hawaii isolates, have a frameshift in *rscS* and do not require the gene for squid colonization or competitive fitness. These same strains have a frameshift in *sypE*, and we provide evidence that this Group A *sypE* allele leads to an upregulation in biofilm activity. This work thus describes the central importance of Syp biofilm in colonization of diverse isolates, and demonstrates that significant evolutionary transitions correspond to regulatory changes in the *syp* pathway.

IMPORTANCE

Biofilms are surface-associated, matrix-encased bacterial aggregates that exhibit enhanced protection to antimicrobial agents. Previous work has established the importance of biofilm formation by a strain of luminous *Vibrio fischeri* bacteria as the bacteria colonize their host, the Hawaiian bobtail squid. In this study, expansion of this work to many natural isolates revealed

that biofilm genes are universally required, yet there has been a shuffling of the regulators of those genes. This work provides evidence that even when bacterial behaviors are conserved, dynamic regulation of those behaviors can underlie evolution of the host colonization phenotype. Furthermore, this work emphasizes the importance of investigating natural diversity as we seek to understand molecular mechanisms in bacteria.

INTRODUCTION

A fundamental question in studying host-associated bacterial communities is understanding how specific microbial taxa assemble reproducibly in their host. Key insights into these processes were first obtained by studying plant-associated microbes, and the discovery and characterization of Nod factors in Rhizobia was valuable to understand how partner choice between microbe and host could be mediated at the molecular level (1, 2). There are complex communities in humans and other vertebrate animals, yet metagenomic and imaging analyses of these communities have revealed striking reproducibility in the taxa present and in the spatial arrangement of those taxa (3–5). Invertebrate animal microbiomes provide appealing systems in which to study microbiome assembly in an animal host: the number of taxa are relatively small, and examination and manipulation of these organisms have yielded abundant information about processes underlying host colonization (6). For this work we focused on the binary symbiosis between *Vibrio fischeri* and bobtail squids, including the Hawaiian bobtail squid, *Euprymna scolopes*. Bobtail squid have an organ for the symbiont termed the light organ, and passage of specific molecules between the newly-hatched host and the symbiont leads to light organ colonization specifically by planktonic *V. fischeri* and not by other bacteria (7–9). The colonization process involves initiation, accommodation, and persistence steps, resulting in light organ crypt colonization by *V. fischeri*. Upon colonization of the squid light organ, bacteria accumulate to high density and produce light. The bacterial light is modulated by the host to

95 camouflage the moonlight shadow produced by the nighttime foraging squid in a cloaking
96 process termed counter-illumination (10, 11). A diel rhythm leads to a daily clearing of 90-95%
97 of the bacteria from the crypts and regrowth of the remaining cells (12). However, the initial
98 colonization process, including biofilm-based aggregation on the host ciliated appendages,
99 occurs only in newly-hatched squid. This work examines regulation of biofilm formation in
100 diverse squid-colonizing *V. fischeri* strains.
101
102 In the well-studied *V. fischeri* strain ES114, biofilm formation is required to gain entry into the
103 squid host. RscS is a hybrid histidine kinase that regulates *V. fischeri* biofilm formation through
104 a phosphorelay involving the hybrid histidine kinase SypF and the response regulator and σ^{54}-
105 dependent activator SypG (13–15). This pathway regulates transcription of the symbiosis
106 polysaccharide (Syp) locus, which encodes regulatory proteins (SypA, SypE, SypF, and SypG),
107 glycosyltransferases, factors involved in polysaccharide export, and other biofilm-associated
108 factors (14, 16). The products of the ES114 *syp* locus direct synthesis and export of a biofilm
109 exopolysaccharide that is critical for colonization. Additional pathways have been identified to
110 influence biofilm regulation in ES114, including the SypE-SypA pathway and inhibition of biofilm
111 formation by BinK and HahK (17–21).
112
113 *V. fischeri* biofilm regulation is connected to host colonization specificity. In the Pacific Ocean,
114 the presence of *rscS* DNA is strongly correlated to the ability to colonize squid (22). As one
115 example, while the fish symbiont MJ11 encodes a complete *syp* locus, it lacks RscS and does
116 not robustly colonize squid. Heterologous expression of ES114 RscS in MJ11 activates the
117 biofilm pathway and is sufficient to enable squid colonization (22). Similarly, addition of ES114
118 RscS to *mjapo*.8.1--a fish symbiont that encodes a divergent RscS that is not functional for
119 squid colonization--allows the strain to colonize squid (22). RscS has also been shown to be
120 necessary for squid colonization in certain strains. In addition to ES114, interruption of *rscS* in

121 *V. fischeri* strains KB1A97 and MJ12 renders them unable to colonize squid. Previous
122 phylogenetic analysis revealed that ancestral *V. fischeri* do not encode *rscS*, and that it was
123 acquired once during the organism's evolution, likely allowing for an expansion in host range.
124 From this analysis, it was concluded that strains with *rscS* can colonize squid, with the only
125 exception being the fish symbionts that harbor the divergent RscS, including *mjapo*.8.1 (22).
126
127 There are similar *Vibrio*-squid associations worldwide, yet only *V. fischeri* and the closely-
128 related *Vibrio logei* have been isolated from light organs (23–26). Our 2009 study revealed that
129 although most symbionts have *rscS* DNA, there are Mediterranean *V. fischeri* (e.g., SR5) that
130 do not have *rscS* yet can colonize squid (22, 24, 27). This unexpected finding prompted the
131 current work to examine whether strains such as SR5 colonize with the known biofilm pathway
132 or with a novel pathway. Here, we show that all *V. fischeri* strains tested require the *syp* locus to
133 colonize a squid host, and we identify two groups of isolates that colonize with novel regulation.
134 Given the exquisite specificity by which *V. fischeri* bacteria colonize squid hosts, this work
135 reinforces the importance of biofilm formation and reveals different regulatory modes across the
136 evolutionary tree.
137
138 **RESULTS**
139
140 **Most *V. fischeri* strains synthesize biofilm in response to RscS overexpression.** Biofilm
141 formation is required for squid colonization, and overexpression of the biofilm regulator RscS in
142 strain ES114 stimulates a colony biofilm on agar plates (15). Our previous work demonstrated
143 that *V. fischeri* strain MJ11 synthesizes a colony biofilm under similar inducing conditions, which
144 is notable because MJ11 does not encode RscS in its chromosome (22). While the ancestral
145 strain MJ11 did not encode RscS, it had what seemed to be an intact *syp* locus, and
146 overexpression of the heterologous RscS from ES114 was sufficient to enable robust squid

147 colonization (22). We examined a phylogenetic tree of *V. fischeri* isolates (Fig. 1), and in this
148 study we expand our analysis of RscS-Syp biofilm regulation in a wider group of *V. fischeri*
149 strains.
150
151 Initially, we asked whether responsiveness to RscS overexpression would yield a similar colony
152 biofilm in this diverse group of strains. We took the same approach as our previous study and
153 introduced plasmid pKG11, which overexpressed ES114 RscS, into strains across the
154 evolutionary tree (22, 28). We observed that almost all strains tested, including those that lack
155 *rscS*, were responsive to overexpression of ES114 RscS (Fig. 2). The morphology of the colony
156 biofilms differed across isolates; but in most cases colony biofilm was evident at 24 h and
157 prominent at 48 h. All of the strains exhibited some wrinkled colony morphology at 48 h with the
158 exception of CG101, which was isolated from the pineapplefish *Cleidopus gloriamaris (25)*.
159 These results demonstrated that most *V. fischeri* strains can produce biofilm in response to
160 RscS overexpression, and this includes strains that presumably have not encountered *rscS* in
161 their evolutionary history.
162
163 One unexpected observation was that there was a subset of *rscS*-encoding strains that were
164 reproducibly delayed in their colony biofilm, and had only a mild wrinkled colony phenotype at
165 48 h (strains MB11B1, ES213, KB2B1; Fig. 2). We considered whether this was due to
166 differential growth of the strains, but resuspension of spots and dilution plating to determine
167 CFU/spot demonstrated no significant growth difference between these strains and ES114
168 under these conditions. The strains are closely-related (Fig. 1) and a previous study had noted
169 that this group shared a number of phenotypic characteristics, e.g. reduced motility in soft agar
170 (29). Those authors termed this tight clade as “Group A” *V. fischeri* (30). Our results in Figure 2
171 argue that Group A strains do not respond to RscS in the same manner as other *V. fischeri*
172 strains, which prompted us to investigate the evolution of the RscS-Syp signaling pathway. We

173 have maintained the Group A nomenclature here, and furthermore we introduce the
174 nomenclature of Group B (a paraphyletic group of strains that contain *rscS*; this group includes
175 the common ancestor of all *rscS*-containing strains) and Group C (a paraphyletic group of
176 strains that contains the common ancestor of all *V. fischeri* - these strains do not contain *rscS*),
177 as shown in Figure 1.
178
179 **Ancestral Group C squid isolates colonize *E. scolopes* independent of RscS and**
180 **dependent on Syp.** Group C strains generally cannot colonize squid, yet there are
181 Mediterranean squid isolates that appear in this group (Fig. 1; (22)). The best-studied of these
182 strains, SR5, was isolated from *Sepiola robusta*, is highly luminous, and colonizes the Hawaiian
183 bobtail squid *E. scolopes* (24). Nonetheless, this strain lacks *rscS* (27). We first asked whether
184 the strain can colonize in our laboratory conditions, and we confirmed that it colonizes robustly,
185 consistent with the result result previously published by Fidopiastis et al. (24) (Fig. 3). Next, we
186 asked whether it uses the Syp biofilm to colonize. To address this question, we deleted the 18
187 kb *syp* locus (i.e., *sypA* through *sypR*) in strains SR5 and ES114. Deletion of *rscS* or the *syp*
188 locus in ES114 led to a substantial defect in colonization, consistent with a known role for these
189 factors (Fig. 3). Similarly, deletion of the *syp* locus in SR5, a strain that does not encode *rscS*,
190 led to a dramatic reduction in colonization (Fig. 3). Therefore, even though strain SR5 does not
191 encode *rscS*, it can colonize squid, and it requires the *syp* locus to colonize normally.
192
193 **RscS is dispensable for colonization in Group A strains.** We noted in the wrinkled colony
194 biofilm assays shown in Figure 2 that Group A strains exhibited a more modest response to
195 overexpression of RscS. Sequencing of the native *rscS* gene in these strains revealed a
196 predicted -1 frameshift (ΔA1141) between the PAS domain and the histidine kinase CA domain.
197 Whereas ES114 and other Group B strains have nine adenines at this position, the Group A
198 strains have eight, leading to a frameshift and then truncation at an amber stop codon, raising

199 the possibility that Group A strains have a divergent biofilm signaling pathway (Fig. 4A). Given
200 the importance of RscS in the Group B strains including ES114, we considered the possibility
201 that this apparent frameshift encoded a functional protein, either through ribosomal
202 frameshifting or through the production of two polypeptides that together provided RscS
203 function; there is precedent for both of these concepts in the literature (31, 32). We first
204 introduced a comparable frameshift into a plasmid-borne overexpression allele of ES114 *rscS*,
205 and this allele did not function with the deletion of the single adenine (Fig. 4B). This result
206 suggested to us that the frameshift in the Group A strains may not be functional. Therefore, we
207 proceeded to delete *rscS* in two Group A strains (MB11B1, ES213) and two Group B strains
208 (ES114, MB15A4). The Group B strains required RscS for squid colonization (Fig. 5A).
209 However, the Group A strains exhibited no deficit in the absence of *rscS* (Fig. 5A). We next
210 attempted a more sensitive assay in which a Group A strain was competed against MB15A4.
211 Previous studies have demonstrated that in many cases Group A strains outcompete Group B
212 strains (30, 33). We competed Group A strain MB11B1 against Group B strain MB15A4 and
213 observed a significant competitive advantage for the Group A strain, as was observed
214 previously (30). Deletion of *rscS* in the Group A strain did not affect competitive fitness,
215 demonstrating that MB11B1 can outcompete a Group B strain even if MB11B1 lacks RscS (Fig.
216 5B).
217
218 **The *syp* locus is broadly required for squid colonization.** Given that Group A strains
219 seemed to represent a tight phylogenetic group in which RscS was not required for colonization
220 or competitive fitness, we next asked whether this group requires the Syp biofilm for
221 colonization. We proceeded to delete the entire *syp* locus in two Group A and two Group B
222 strains and to conduct single-strain colonization analysis. In each strain assayed, the *syp* locus
223 was required for full colonization, and we observed a 2-4 log reduction in CFU per animal in the
224 absence of the *syp* genes, pointing to a critical role for Syp biofilm in these strains (Fig. 6). In

225 Group A strains in particular, no colonization was detected in the absence of the *syp* locus.
226 Additionally, we isolated a transposon insertion in SR5 *sypJ*, and this strain did not colonize
227 squid well, arguing that this effect is due to the Syp biofilm and not due to regulation of a distinct
228 phenotype by regulators within the locus.
229
230 **Group A strains encode an alternate allele of SypE.** It seemed curious to us that Group A
231 strains do not encode a functional RscS and do not require *rscS* for colonization, yet in many
232 cases Group A strains can outcompete Group B strains (e.g. MB11B1 in Fig. 5B; and Refs. (30,
233 33)). We reasoned that if the Syp biofilm had a different regulatory architecture in Group A
234 strains--e.g., constitutively activated or activated by a different regulatory protein--then this could
235 explain the Syp regulation independent of RscS. Genome sequencing of SR5 and MB11B1 did
236 not identify a unique histidine kinase that was likely to directly substitute for RscS (27, 33).
237 Given that the *syp* locus encodes biofilm regulatory proteins, we examined *syp* conservation.
238 We used TBLASTN with the ES114 Syp proteins as queries to determine amino acid
239 conservation in the other *V. fischeri* Group A strain MB11B1, Group C strain SR5, and the *Vibrio*
240 *vulnificus* type strain ATCC 27562 (34, 35). As shown in Figure 7, ES114 SypE, a response
241 regulator and serine kinase/phosphatase that is a negative regulator of the Syp biofilm (17, 36),
242 exhibited the lowest level of conservation among *syp* locus products. *V. vulnificus* does not
243 encode a SypE ortholog (37), as the syntenic (but not homologous) RbdE encodes a predicted
244 ABC transporter substrate-binding protein. The closest hit for SypE was AOT11_RS12130 (9%
245 identity), compared to 7% identity for the RbdE. Due to the reduced conservation at both the
246 strain and species levels, we analyzed *V. fischeri* MB11B1 SypE in greater detail. Examination
247 of the *sypE* coding sequence revealed an apparent -1 frameshift mutation in which the position
248 33 (guanine in ES114 and adenine in other Group B and C strains examined) is absent in Group
249 A strains (Fig. 7B). We therefore considered the hypothesis that SypE is nonfunctional in Group

250 A, and that these strains can colonize because they are lacking a functional copy of this
251 negative regulator that is itself regulated by RscS.
252
253 To test this hypothesis, we relied on knowledge of the biofilm regulatory pathway from ES114, in
254 which overexpression of SypG produces a wrinkled colony phenotype, but only in strains lacking
255 SypE activity (38, 39). Therefore, we introduced the SypG-overexpressing plasmid pEAH73 into
256 strains as a measure of whether the SypE pathway was intact. In the ES114 strain background,
257 we observed cohesive wrinkled colony formation at 48 h in an ES114 Δ*sypE* strain, but not in
258 the wild-type parent (Fig. 8A). If the *sypE* frameshift observed in MB11B1 led to a loss of
259 function, then introduction of that frameshift into ES114 would lead to a strain that is equivalent
260 to the Δ*sypE* strain. We constructed this strain and upon SypG overexpression we observed
261 wrinkled colony formation. Surprisingly, the biofilm phenotype was observed earlier (i.e., by 24
262 h) and leads to more defined colony biofilm architecture at 48 h. While the lack of SypE leads to
263 increased and more rapid biofilm formation, in this assay we observed an even greater increase
264 as a result of the frameshift in *sypE* (Fig. 8A).
265
266 We proceeded to conduct a similar assay in the MB11B1 strain background. The colony biofilm
267 phenotypes were muted compared to the ES114 background, but the pattern observed is the
268 same. Strains lacking the additional nucleotide at position 33 (i.e., the native MB11B1 allele)
269 exhibited the strongest cohesion, whereas strains with the nucleotide to mimic ES114 *sypE* (i.e.,
270 added back in MB11B1 *sypE*(nt::33G)) were not cohesive (Fig. 8B). These results argue that a
271 novel allele of *sypE* is found in Group A strains and this allele results in more substantial biofilm
272 formation than in a Δ*sypE* strain.
273
274 Our finding that the MB11B1 *sypE* allele promotes biofilm formation bolstered the model that
275 this allele contributes to the ability of MB11B1 to colonize squid independent of RscS. To test

276 this model, we introduced the frameshift into ES114 or “corrected” the frameshift in MB11B1.
277 We then conducted single-strain colonization assays, and in each case the *sypE* allele alone
278 was not sufficient to alter the overall colonization behavior of the strain (Fig. 9). Therefore, these
279 data suggest that the frameshift in the MB11B1 *sypE* is not sufficient to explain its ability to
280 colonize independent of RscS, and therefore other regions of SypE and/or other loci in the
281 MB11B1 genome contribute to its ability to colonize independent of RscS.
282
283 **BinK is active in Group A, B, and C strains.** We recently described the histidine kinase, BinK,
284 which negatively regulates *syp* transcription and Syp biofilm formation (18). In ES114,
285 overexpression of BinK impairs the ability of *V. fischeri* to colonize. We therefore reasoned that
286 if BinK could function in Group A strains and acted similarly to repress Syp biofilm, then
287 overexpression of BinK would reduce colonization of these strains. We introduced the pBinK
288 plasmid (i.e., ES114 *binK* (18)) and asked whether multicopy *binK* would affect colonization. In
289 strain MB11B1, BinK overexpression led to a dramatic reduction in colonization (Fig. 10A).
290 Therefore, there is a clear effect for BinK overexpression on the colonization of the Group A
291 strain MB11B1.
292
293 We attempted to ask the same question in Group C strain SR5, but the pES213-origin plasmids
294 were not retained during squid colonization. Therefore, we instead asked whether deletion of
295 the BinK, a negative regulator of ES114 colonization, has a comparable effect in SR5 (18). We
296 deleted *binK* and observed a 2.4-fold competitive advantage during squid competition (Fig.
297 10B), arguing that BinK in this Group C strain is active and performs an inhibitory function
298 similar to that in ES114.
299
300 We next examined the colony biofilm phenotype for strains lacking BinK. MB11B1 Δ*binK*
301 exhibited a mild colony biofilm phenotype at 48 h, as evidenced by the cohesiveness of the spot

302 when disrupted with a toothpick (Fig. 10C). The colonies also exhibited an opaque phenotype.
303 In a minority of experimental replicates, wrinkled colony morphology was evident at 48 h, but in
304 all samples wrinkled colony morphology was visible at 7 d (data not shown). The SR5 Δ*binK*
305 strain also exhibited slightly elevated biofilm morphology at 48 h, though the cells were not as
306 cohesive as those of MB11B1 Δ*binK* (Fig. 10C). Together, the results in Figure 10 argue that
307 BinK, a factor that has been characterized as a negative regulator of Syp biofilm, plays similar
308 roles in Group A and Group C strains and has a widely-conserved function across the *V. fischeri*
309 evolutionary tree.
310
311 **DISCUSSION**
312
313 This study examines regulation of a beneficial biofilm that is critical to host colonization
314 specificity in *V. fischeri.* The Syp biofilm was discovered thirteen years ago and has been
315 characterized extensively for its role in facilitating squid colonization by *V. fischeri.* This work
316 establishes that the *syp* locus is required broadly across squid symbionts, and it uncovers three
317 groups of *V. fischeri* that use different regulatory programs upstream of the *syp* locus. A
318 simplified phylogenetic tree showing key features of squid symbionts in these three groups is
319 shown in Figure 11.
320
321 There are three nested evolutionary groups of *V. fischeri* that have been described separately in
322 the literature and here we formalize the nomenclature of Groups C, B, and A. Group A is a
323 monophyletic group, as are Groups AB and ABC (Fig. 1). This work provides evidence that
324 squid symbionts in each group have a distinct biofilm regulatory architecture. Most *V. fischeri*
325 isolates that have been examined from the ancestral Group C cannot colonize squid; however,
326 those that can colonize do so without the canonical biofilm regulator RscS. We show that the
327 known targets of RscS regulation—genes in the *syp* biofilm locus—are nonetheless required for

328 squid colonization by this group. Group B strains include the well-characterized ES114 strain,
329 which requires RscS and the *syp* locus to colonize squid. Group A strains differ phenotypically
330 and behaviorally from the sister Group B strains (30), and we demonstrate that these strains
331 have altered biofilm regulation. Group A strains have a frameshift in *rscS* that renders it
332 nonfunctional, and a 1 bp deletion in *sypE*, and we provide evidence that the *sypE* allele
333 promotes biofilm development in the absence of RscS. Additionally, we note that the *sypE*
334 frameshift is not present in SR5, arguing for distinct modes of biofilm regulation in Groups A, B,
335 and C.
336
337 At the same time, this study provides evidence that some aspects of biofilm regulation are
338 conserved in diverse squid symbionts, such as the effects of the strong biofilm negative
339 regulator BinK. Published data indicate that evolved BinK alleles can alter colonization of H905
340 (Group B) and MJ11 (Group C), and that a deletion of MJ11 *binK* leads to enhanced
341 colonization (20). Our experiments in Figure 10 show a clear effect for BinK in all three
342 phylogenetic groups. We also observed responsiveness to RscS overexpression in all squid
343 symbionts examined (Fig. 2). CG101 was the only *V. fischeri* strain examined that did not exhibit
344 a colony biofilm in response to RscS overexpression. CG101 was isolated from the Australian
345 fish *Cleidopus gloriamaris*; based on these findings, we suspect that the strain does not have an
346 intact *syp* locus or otherwise has divergent biofilm regulation.
347
348 It remains a formal possibility that the entire *syp* locus is not required in Group A or Group C,
349 but instead that only one or a subset of genes in the locus are needed. We have constructed
350 Campbell-type (insertion duplication) alleles to interrupt *sypG* in MB11B1 and SR5, and
351 additionally have isolated a transposon insertion in SR5 *sypJ*, and none were able to colonize
352 well. Additionally, aggregation in squid mucus has been observed for the Group A strain
353 MB13B2, and this aggregation is dependent on *sypQ* (40). In our data we note that Group A

354 strains were completely unable to colonize in the absence of the *syp* locus, unlike the tested
355 Group B & C strains that exhibited reduced colonization in their respective mutants (Figs. 3, 6).
356 Therefore, the simplest explanation is that the *syp* locus is required in divergent strains in a
357 manner similar to how it is used in ES114. We think that the ability to completely delete the *syp*
358 locus is a clean way to ask whether the locus is required for specific phenotypes, and our
359 strains are likely to be useful tools in probing Syp protein function in diverse *V. fischeri* isolates.
360
361 It is intriguing to speculate as to how the two frameshifts in the Group A strains arose, and why
362 the nonfunctional RscS is tolerated in this group. One possible scenario is that the Group A
363 strains acquired a new regulatory input into the Syp pathway, and that the presence of this new
364 regulator bypassed the requirement for RscS. We note that comparative genomic analysis of
365 Hawaiian D (dominant)-type strains--which largely overlap with Group A--revealed an additional
366 250 kb of genomic DNA compared to other isolates, yielding a large cache of genes that could
367 play a role in this pathway (33). A related possibility is that *rscS*-independent colonization
368 results from altered regulation of the *syp* locus, either due to changes in regulators (e.g. SypF)
369 or sites that are conserved with Group B. An additional possibility is that the *sypE* frameshift
370 arose, enabling Group A strains to colonize independent of *rscS*. Given that correction of this
371 frameshift in MB11B1 does not significantly affect colonization ability (Fig. 9), this sequence of
372 events seems less likely, and we expect that another regulator in MB11B1 is required for the
373 RscS-independent colonization phenotype. There is evidence that under some conditions LuxU
374 can regulate the *syp* biofilm (41), and as this protein is conserved in *V. fischeri* it may play an
375 important role in Group A or Group C.
376
377 Results from two experimental conditions suggest that the Group A strains may have an
378 elevated baseline level of biofilm formation. Our data indicate that in the absence of BinK or
379 upon SypG overexpression, MB11B1 colonies exhibit strong cohesion under conditions in which

380 ES114 does not (Figs. 8, 10). Furthermore, we note that the Group A strain MB11B1, when
381 lacking BinK, also exhibits a darker, or more opaque, colony phenotype (Fig. 10). This
382 phenotype has been observed in some ES114 mutants (16) but not in the corresponding ES114
383 Δ*binK* strain (Fig. 10). The entire colonization lifecycle likely requires a balance between biofilm
384 formation/cohesion and biofilm dispersal, and these data argue that Group A strains may be
385 more strongly tilted toward the biofilm-producing state. There is evidence that strains lacking
386 BinK exhibit a colonization advantage in the laboratory (18, 20), suggesting that this strategy of
387 more readily forming biofilms may provide a fitness advantage in nature. At the same time, the
388 biofilm negative regulator BinK is conserved among *V. fischeri* strains examined (including
389 MB11B1; Fig. 10), arguing that there is a benefit to reducing biofilm formation under some
390 conditions.
391
392 Our study provides hints as to the role of SypE in MB11B1 and other Group A strains. In ES114,
393 the C-terminus is a PP2C serine kinase domain, whereas the N-terminus of SypE is an RsbW
394 serine phosphatase domain. SypE acts to phosphorylate and dephosphorylate SypA Ser-56,
395 with the unphosphorylated SypA being the active form to promote biofilm development (17). The
396 balance between SypE kinase and phosphatase is modulated by a central two-component
397 receiver domain (17). Our data that the MB11B1 *sypE* allele promotes biofilm formation suggest
398 that the protein is tilted toward the phosphatase activity. In MB11B1, the frameshift early in *sypE*
399 suggests that there is a different start codon and therefore a later start codon. An alternate GTG
400 start codon in MB11B1 occurs corresponding to codon 18 in ES114 *sypE* (Fig. 7), and this is
401 likely the earliest start for the MB11B1 polypeptide. We attempted to directly identify the SypE
402 N-terminus by mass spectrometry, yet we could not identify the protein from either strain.
403 Additional study is required to elucidate how MB11B1 SypE acts to promote biofilm formation.
404

405 *V. fischeri* strains are valuable symbionts in which to probe the molecular basis to host
406 colonization specificity in animals (22, 25, 26). A paradigm has emerged in which biofilm
407 formation through the RscS-Syp pathway is required for squid colonization but not for fish
408 colonization. This study affirms a role of the Syp biofilm, but at the same time points out
409 divergent (RscS-independent) regulation in Group C and Group A isolates. In another well-
410 studied example of symbiotic specificity, Rhizobial Nod factors are key to generating specificity
411 with the plant host, yet strains have been identified that do not use this canonical pathway (42,
412 43). Future work will elaborate on these RscS-independent pathways to determine how non-
413 canonical squid colonization occurs in diverse natural isolates.
414
415 **MATERIALS & METHODS**
416
417 **Bacterial strains and growth conditions**. *V. fischeri* and *E. coli* strains used in this study can
418 be found in Table 1. *E. coli* strains, used for cloning and conjugation, were grown in Luria-
419 Bertani (LB) medium (25 g Difco LB Broth [BD] per liter). *V. fischeri* strains were grown in Luria-
420 Bertani salt (LBS) medium (25 g Difco LB Broth [BD], 10 g NaCl, and 50 ml 1 M Tris buffer pH
421 7.0, per liter). Growth media were solidified by adding 15 g Bacto agar (BD) per liter. When
422 necessary, antibiotics (Gold Biotechnology) were added at the following concentrations:
423 tetracycline, 5 µg/ml for *V. fischeri*; erythromycin, 5 µg/ml for *V. fischeri*; kanamycin, 50 µg/ml for
424 *E. coli* and 100 µg/ml for *V. fischeri*; and chloramphenicol, 25 µg/ml for *E. coli*, 2.5 -5 µg/ml for
425 Group B *V. fischeri*, and 1 - 2.5 µg/ml for Group A *V. fischeri*. The two MB11B1 / pKV69 strains
426 listed reflect two separate constructions of this strain, though we have not identified any
427 differences between them.
428
429 **Phylogenetic analysis.** Phylogenetic reconstructions assuming a tree-like topology were
430 created with three methods: maximum parsimony (MP); maximum likelihood (ML); and

431 Bayesian inference (Bayes) as previously described (22, 30). Briefly, MP reconstructions were
432 performed by treating gaps as missing, searching heuristically using random addition, tree-
433 bisection reconnection with a maximum of 8 for swaps, and swapping on best only with 1000
434 repetitions. For ML and Bayesian analyses, likelihood scores of 1500+ potential evolutionary
435 models were evaluated using both the corrected and uncorrected Akaike Information Criterion,
436 the Bayesian Information Criterion, and Decision Theory (Performance Based Selection) as
437 implemented by jModelTest2.1 (44). For all information criteria, the most optimal evolutionary
438 model was a symmetric model with a proportion of invariable sites and a gamma distribution of
439 rate heterogeneity (SYM+I+Γ).
440
441 ML reconstruction was implemented via PAUP*4.0a163 (45) by treating gaps as missing,
442 searching heuristically using random addition, tree-bisection reconnection for swaps, and
443 swapping on best only with 1000 repetitions. Bayesian inference was done by invoking the
444 'nst=6' and 'rates=invgamma' and 'statefreqpr=fixed(equal)' settings in the software package
445 MrBayes3.2.6 (46). The Metropolis-coupled Markov chain Monte Carlo (MCMCMC) algorithm
446 used to estimate the posterior probability distribution for the sequences was set up with
447 'temp=0.2' and one incrementally 'heated' chain with three 'cold' chains; these four chains were
448 replicated two times per analysis to establish convergence of the Markov chains (i.e.,
449 'stationarity' as defined by (47) and interpreted previously in (30)). For this work, stationarity was
450 achieved after approximately 50,000 samples (5,000,000 generations) were collected, with 25%
451 discarded. The ~37,500 samples included were used to construct a 50% majority-rule
452 consensus tree from the sample distribution generated by MCMCMC and assess clades'
453 posterior probabilities. For ML and MP analyses, the statistical confidence in the topology of
454 each reconstruction was assessed using 1000 bootstrap replicates. Phylogenetic trees were
455 visualized with FigTree 1.4.3 (http://tree.bio.ed.ac.uk/software/figtree); the final tree was edited
456 for publication with Inkscape 0.91 (http://inkscape.org/) and GIMP 2.8.22 (http://www.gimp.org/).

457

458 **DNA synthesis and sequencing.** Each of the primers listed in Table 3 was synthesized by
459 Integrated DNA Technologies (Coralville, IA). Full inserts from all cloned constructs were
460 verified by Sanger DNA sequencing through ACGT, Inc via the Northwestern University
461 Feinberg School of Medicine NUSeq Core Facility; or the University of Wisconsin-Madison
462 Biotechnology Center. Sequence data was analyzed with SeqMan Pro (DNAStar software),
463 SnapGene (GSL Biotech), and Benchling.

464

465 **Construction of gene deletions.** Deletions in *V. fischeri* strains ES114 and MB11B1 were
466 made according to the lab's gene deletion protocol: doi:10.5281/zenodo.1470836. In brief, 1.6
467 kb upstream and 1.6 kb downstream of the targeted gene or locus were cloned into linearized
468 plasmid pEVS79 (amplified with primers pEVS79_rev_690/pEVS79_for_691) using Gibson
469 Assembly (NEBuilder HiFi DNA Assembly cloning kit) with the primer combinations listed in
470 Table S1. The Gibson mix, linking together the upstream and downstream flanking regions, was
471 transformed into *E. coli* on plates containing X-gal, with several white colonies selected for
472 further screening by PCR using primers flanking the upstream/downstream junction (Tables 3
473 and S1). The resulting plasmid candidate was confirmed by sequencing and conjugated into the
474 *V. fischeri* recipient by tri-parental mating with helper plasmid pEVS104, selecting for the
475 chloramphenicol resistance of the plasmid backbone. *V. fischeri* colonies were first screened for
476 single recombination into the chromosome by maintaining antibiotic resistance in the absence of
477 selection and then screened for double recombination by the loss of both the antibiotic resistant
478 cassette and the gene/locus of interest. Constructs were verified by PCR (Table 3) and
479 sequencing.

480

481 Deletion of SR5 *binK* was conducted using Splicing by Overlap Extension PCR (SOE-PCR) and
482 natural transformation (method modified from (48)). Oligos binK-F1 and binK-R1-LUH, and

483 oligos binK-F2-RUH and binK-R2 were used in a PCR with MJM1125 (SR5) genomic DNA as
484 the template to amplify DNA fragments containing ~1 kb of sequence upstream and
485 downstream relative to *binK*, respectively. Using SOE-PCR, these fragments were fused on
486 either side to a third DNA fragment containing an Erm^R cassette, which was amplified using
487 pHB1 as template and oligos HB41 and HB42. We then used natural transformation with
488 pLostfoX (49) to insert this mutagenic DNA into MJM1125, where the flanking sequences guide
489 the Erm^R cassette to replace *binK*, generating the desired gene deletion. Candidate SR5 Δ*binK*
490 mutants were selected after growth on LBS-Erm5 plates. Oligos binK-F1 and binK-R2, and HB8
491 and binK-FO were used to screen candidates for the correct deletion scar by PCR, and oligos
492 KMB_036 and KMB_037 were used to confirm the absence of *binK* in the genome. The deletion
493 was verified by Sanger sequencing with primers HB8, HB9, HB42, and HB146. The base
494 plasmid pHB1 contains an erythromycin resistance cassette flanked by FRT sites, and was
495 constructed using oligos HB23 and HB39 with gBlock gHB1 (sequence in Supplementary File
496 S1; Integrated DNA Technologies, Inc.) as template to amplify the Erm^R cassette flanked by
497 HindIII and BamHI sites, which was then cloned into the corresponding site in pUC19.
498
499 For most constructs, the deleted genetic material was between the start codon and last six
500 amino acids (50), with two exceptions: the Δ*sypE* in MJM1130 included the ATG that is two
501 amino acids upstream of the predicted start codon, but not the canonical start codon; and the
502 Δ*binK* alleles in MJM1117, MJM1130, and MJM2114, which were constructed to be equivalent
503 to MJM2251 (Δ*binK* in ES114) (18). The Δ*binK* alleles in these strains include the start codon,
504 the next six codons, two codons resulting from ATCGAT (ClaI site), and the last three codons
505 for a predicted 12 amino acid peptide.
506
507 **Construction of *sypE* alleles.** To create *sypE*(ntG33Δ) in MJM1100 and *sypE*(nt33::G) in
508 MJM1130, the single point mutation was created by amplifying the gene in two halves, with the

509 N-terminal portion consisting of approximately 300 bp upstream of *sypE* up through nucleotide
510 33 and the C-terminal portion consisting of nucleotide 33 and the remaining *sypE* gene. The
511 overlap between the two halves contained the single nucleotide polymorphism in the primers
512 that connected them. The altered *sypE* alleles were initially cloned into plasmid pEVS107
513 (linearized with primers pEVS107_3837/pEVS107_3838) using Gibson Assembly and then the
514 entire altered *sypE* allele was subcloned into pEVS79 with Gibson Assembly (Table S1). After
515 double recombination of the vector into *V. fischeri*, candidate colonies for the altered *sypE* in
516 MJM1100 were screened with primers ES114_indel_for/ES114_indel_rev. The primer set
517 anneals more strongly to the wildtype *sypE* sequence than to *sypE*(ntG33::Δ). Candidates in the
518 MJM1100 background with a fainter PCR band were sequenced and confirmed to have the
519 *sypE*(ntG33::Δ) allele. For MJM1130, the primer set MB11B1_indel_for/MB11B1_indel_rev
520 anneals more strongly to the *sypE*(nt33::G) allele than to the naturally occurring *sypE* allele and
521 candidates in MJM1130 that contained a more robust PCR band were selected for sequencing
522 to be confirmed as being *sypE*(nt33::G).
523
524 **Construction of pKG11 *rscS1*(ntA1141::Δ)**. Plasmid pKG11 encodes an overexpression allele
525 of RscS, termed *rscS1 (15, 28)*. *rscS* nucleotide A1141 was deleted on the plasmid using the
526 Stratagene Quikchange II Site-Directed Mutagenesis Kit with primers rscS_del1F and
527 rscS_del1R. The resulting plasmid, pMJM33, was sequenced with primers MJM-154F and
528 MJM-306R to confirm the single base pair deletion.
529
530 **Squid colonization**. Hatchling *E. scolopes* were colonized by exposure to approximately 3 x
531 10^3 CFU/ml (ranging from 5.2 x 10^2 - 1.4 x 10^4 CFU/ml; as specified in figure legends) of each
532 strain in a total volume of 40 ml of FSIO (filter-sterilized Instant Ocean) for 3 hours. Squid were
533 then transferred to 100 ml of FSIO to stop the inoculation and then transferred to 40 ml FSIO for
534 an additional 45 hours with a water change at 24 hours post inoculation. For Figure 10A,

535 kanamycin was added to the FSIO to keep selective pressure on the plasmid. After 48 hours of
536 colonization, the squid were euthanized and surface sterilized by storage at -80 ºC, according to
537 standard practices (51). For determination of CFU per light organ, hatchlings were thawed,
538 homogenized, and 50 µl of homogenate dilutions was plated onto LBS plates. Bacterial colonies
539 from each plate were counted and recorded. Mock treated, uncolonized hatchlings ("apo-
540 symbiotic") were used to determine the limit of detection in the assay. The competitive index
541 (CI) was calculated from the relative CFU of each sample in the output (light organ) versus the
542 input (inoculum) as follows:
543 Log_{10} ((Test strain[light organ] / Control strain[light organ]) / (Test strain[inoculum] / Control
544 strain[inoculum])). For competitions of natural isolates, the Group A strain (or its Δ*rscS*
545 derivative) was the test strain and the Group B strain was the control strain. Colony color was
546 used to enumerate colonies from each--white for Group A strains MB11B1 and ES213; yellow
547 for Group B strains ES114 and MB15A4--along with PCR verification of selected colonies. For
548 competition between SR5 and SR5 Δ*binK*, 100 colonies per squid were patched onto LBS-Erm5
549 and LBS.
550
551 **Colony biofilm assays**. Bacterial strains were grown in LBS media (Fig. 10C) or LBS-Cam2.5
552 media (Figs. 2, 8) for approximately 17 hours, then 10 µl (Fig. 2) or 8 µl (Fig. 8, 10C) was
553 spotted onto LBS plates (Fig. 10C) or LBS-Tet5 plates (Figs. 2, 8). Spots were allowed to dry
554 and the plates incubated at 25 °C for 48 hours. Images of the spots were taken at 24 and 48 h
555 post-spotting using a Leica M60 microscope and Leica DFC295 camera. After 48 h of growth,
556 the spots were disrupted using a flat toothpick and imaged similarly.
557
558 **Analysis of DNA and protein sequences *in silico***. Amino acid sequences for *V. fischeri*
559 ES114 *syp* genes were obtained from RefSeq accession NC_006841.2. Local TBLASTN
560 queries were performed for each protein against nucleotide databases for the following strains,

561 each of which were derived from the RefSeq cds_from_genomic.fna file: *V. fischeri* SR5
562 (GCA_000241785.1), *V. fischeri* MB11B1 (GCA_001640385.1) and *V. vulnificus* ATCC27562
563 (GCA_002224265.1). Percent amino acid identity was calculated as the identity in the BLAST
564 query divided by the length of the amino acid sequence in ES114. Domain information is from
565 the PFAM database (52).
566
567 **FIGURE LEGENDS**
568 **Figure 1. *Vibrio fischeri* phylogeny, highlighting the source of each strain**. Bayesian
569 phylogram (50% majority-rule consensus) inferred with a SYM+I+Γ model of evolution for the
570 concatenated gene fragments *recA*, *mdh*, and *katA*. In this reconstruction, the root connected to
571 a clade containing the four non-*V. fischeri* outgroup taxa. Statistical support is represented at
572 nodes by the following three numbers: upper left, Bayesian posterior probability (of
573 approximately 37,500 non-discarded samples) multiplied by 100; upper right, percentage of
574 1000 bootstrap Maximum Likelihood pseudo-replicates; bottom middle center, percentage of
575 1000 bootstrap Maximum Parsimony pseudo-replicates. Statistical support values are listed only
576 at nodes where more than 2 methods generated support values ≥ 50%. Strains sharing identical
577 sequences for a given locus fragment are listed next to a vertical bar at a leaf; because of a lack
578 of space, some support values have been listed either immediately to the right of their
579 associated nodes and are marked with italicized lower-case Roman numerals in the phylogram.
580 The isolation habitat and geography of each strain are indicated by symbol and color,
581 respectively. The black bar represents 0.01 substitutions/site.
582
583 **Figure 2. Most *V. fischeri* strains tested form colony biofilm in response to RscS**
584 **overexpression.** Spot assays of the indicated *V. fischeri* strains carrying pKV69 (vector) or
585 pKG11 (*rscS1*; overexpressing ES114 *rscS*) after 24 and 48 h. Strains are MJM1268,
586 MJM1269, MJM1246, MJM1247, MJM1266, MJM1267, MJM1219, MJM1221, MJM1238,

587 MJM1239, MJM1104, MJM1106, MJM1276, MJM1277, MJM1270, MJM1271, MJM1258,
588 MJM1259, MJM1254, MJM1255, MJM1242, MJM1243, MJM1240, MJM1241, MJM1272,
589 MJM1273, MJM1274, MJM1275, MJM1278, MJM1279, MJM1109, MJM1111, MJM1280,
590 MJM1281, MJM1260, MJM1261, MJM1244, MJM1245, MJM1256, and MJM1257. Different
591 phenotypes were observed in the isolates examined; in most cases we observed wrinkled
592 colonies, but in some cases we observed only a subtle pocked pattern (EM30), and in other
593 cases we did not observe any change in colony morphology compared to the vector control
594 (noted by *). The black bar is 5 mm in length.
595
596
597 **Figure 3. Squid colonization in Group C strain SR5, which does not encode RscS, is**
598 **dependent on the *syp* polysaccharide locus**. Single-strain colonization experiments were
599 conducted and circles represent individual animals. The limit of detection for this assay,
600 represented by the dashed line, is 7 CFU/LO, and the horizontal bars represent the median of
601 each set. Hatchling squid were inoculated with 1.5-3.2 × 10^3 CFU/ml bacteria, washed at 3 h
602 and 24 h, and assayed at 48 h. Each dot represents an individual squid. Strains are: MJM1100,
603 MJM3010, MJM3062, MJM1125, and MJM3501. Statistical comparisons by the Mann-Whitney
604 test, ** $p<0.01$, *** $p<0.001$, **** $p<0.0001$.
605
606 **Figure 4. Group A strains have a frameshift in *rscS***. (A) ES114 RscS protein domains.
607 Nucleotides 1114-1173 in ES114 RscS (AF319618) and their homologous sequences in the
608 other Group B and Group A strains are listed. The -1 frameshift is present in the Group A *rscS*
609 alleles. The ES114 reading frame is noted on the top of the alignment and the Group A reading
610 frame on the bottom, which is predicted to end at the amber stop codon. (B) Deletion of
611 nucleotide A1141 in ES114 to mimic this frameshift in pKG11 renders it unable to induce a
612 colony biofilm in a spot assay at 48 h. Strains are MJM1104, MJM1106, and MJM2226.

613

614 **Figure 5. Group A strains MB11B1 and ES213 do not require RscS for squid colonization**.
615 Wild-type (WT) and Δ*rscS* derivatives of the indicated strains were assayed in (A) a single-strain
616 colonization assay and (B) competitive colonization against Group B strain MB15A4. Hatchling
617 squid were inoculated at 3.5-14 × 10^3 CFU/ml bacteria, washed at 3 h and 24 h, and assayed at
618 48 h. Each dot represents an individual squid. (A) Strains: MJM1100, MJM3010, MJM2114,
619 MJM3042, MJM1130, MJM3046, MJM1117, and MJM3017. The limit of detection is represented
620 by the dashed line, and the horizontal bars represent the median of each set. In both panels,
621 open dots are wild type and filled dots are Δ*rscS*. (B) The competitive index (CI) is defined in the
622 methods and is shown on a Log_{10} scale. Strains: MJM1130 and MJM3046, each competed
623 against MJM2114. Values greater than 1 indicate more MB11B1. Statistical comparisons by the
624 Mann-Whitney test, ns not significant, **** $p<0.0001$.

625

626 **Figure 6. Group B and Group A strains require the *syp* locus for robust squid**
627 **colonization**. Wild type (WT) and Δ*syp* derivatives of the indicated strains were assayed in a
628 single strain colonization assay. Hatchling squid were inoculated with 6.7-32 × 10^2 CFU/ml
629 bacteria (ES114 and MB15A4 backgrounds) or 5.2-8.9 × 10^2 CFU/ml bacteria (MB11B1 and
630 ES213 backgrounds), washed at 3 h and 24 h, and assayed at 48 h. Each dot represents an
631 individual squid. The limit of detection is represented by the dashed line and the horizontal bars
632 represent the median of each set. Strains are MJM1100, MJM3062, MJM2114, MJM3071,
633 MJM1130, MJM3065, MJM1117, and MJM3068. Statistical comparisons by the Mann-Whitney
634 test, **** $p<0.0001$.

635

636 **Figure 7. Group A strains have a frameshift in *sypE***. (A) Amino acid identity in the Syp locus.
637 Results show the identity from TBLASTN query using the *V. fischeri* ES114 protein sequences
638 as queries against genes in the homologous loci in *V. fischeri* strains or *V. vulnificus* ATCC

639 27562. The identity for SypE against *V. vulnificus* is plotted for the syntenous RbdE, although
640 this is not the highest TBLASTN hit, as described in the text. (B) ES114 SypE protein domains.
641 Nucleotides 1-60 in ES114 *sypE* and their homologous sequences in the other Group C, B, and
642 A strains are listed. A -1 frameshift is present in the Group A *sypE* alleles. The ES114 reading
643 frame is noted on the top of the alignment and the Group A reading frame on the bottom, which
644 is predicted to end at the amber stop codon. A possible GTG start codon for the resumption of
645 translation in the ES114 reading frame is present at the position corresponding to the 18th
646 codon in ES114 *sypE*.
647
648 **Figure 8. The MB11B1 *sypE* frameshift leads to an enhanced biofilm phenotype upon**
649 **SypG overexpression**. Spot assays of strains carrying the pKV69 vector or pEAH73 SypG
650 overexpression plasmid. (A) ES114 strain background. Strains lacking SypE produce a wrinkled
651 colony phenotype upon SypG overexpression. Deletion of nucleotide 33 in *sypE* to mimic the
652 Group A frameshift led to earlier wrinkling and a more pronounced colony biofilm at 48 h.
653 Strains: MJM1104, MJM3455, MJM3418, MJM3419, MJM3364, and MJM3365. (B) Group A
654 strain MB11B1, which naturally carries a -1 frameshift in *sypE*, exhibits a cohesive phenotype at
655 48 h with overexpression of SypG. Deletion of *sypE* reduces this phenotype, and repairing the
656 frameshift by addition of a guanosine at nucleotide 33 further reduces the cohesiveness of the
657 spot. Strains: MJM3370, MJM3371, MJM3411, MJM3412, MJM3398, and MJM3399.
658
659 **Figure 9. The *sypE* -1 frameshift allele is not sufficient to affect colonization ability**. The
660 indicated strains were assayed in a single-strain colonization assay. Gray boxes denote alleles
661 distinct from their wild-type background. Frameshift “fs” refers to alleles--relative to an ES114
662 reference--that lack *rscS* nucleotide A1141, or that lack *sypE* nucleotide G33. The wild-type
663 MB11B1 strain contains natural frameshifts in these loci, and the ES114 nt33::ΔG allele was
664 constructed. Addition back of the nucleotide in MB11B1 *sypE* is denoted as “(+)”. Hatchling

665 squid were inoculated with 6.8-8.4 × 10^2 CFU/ml bacteria (MB11B1 background) or 4.0-5.4 ×
666 10^3 CFU/ml bacteria (ES114 background), washed at 3 h and 24 h, and assayed at 48 h. Each
667 dot represents an individual squid. The limit of detection is represented by the dashed line and
668 the horizontal bars represent the median of each set. Strains are MJM1100, MJM3010,
669 MJM4323, MJM3394, MJM1130, and MJM3397. Statistical comparisons by the Mann-Whitney
670 test, ns not significant.
671
672 **Figure 10. BinK is active in Groups A, B, and C**. (A) Overexpression of pBinK inhibits
673 colonization in Group A strain MB11B1. Hatchling squid were inoculated with 3.6-6.8 × 10^3
674 CFU/ml bacteria, washed at 3 h and 24 h, and assayed at 48 h. Each dot represents an
675 individual squid. The limit of detection is represented by the dashed line and the horizontal bars
676 represent the median of each set. The vector control is pVSV104. Strains are MJM1782,
677 MJM2386, MJM2997, and MJM2998. (B) Deletion of *binK* confers a colonization defect in Group
678 C strain SR5. Strains are MJM1125 and MJM3571; mean inoculum of 7.2 × 10^3 CFU/ml;
679 median competitive index (CI) was 0.38 (i.e., 2.4-fold advantage for the mutant). (C) Deletion of
680 the native *binK* in MB11B1 yielded opaque and cohesive spots, which are stronger phenotypes
681 than we observe in ES114. Strains are MJM1100, MJM2251, MJM1130, MJM3084, MJM2997,
682 and MJM2998. Statistical comparisons by the Mann-Whitney test, **** $p<0.0001$.
683
684 **Figure 11. Summary model of distinct modes of biofilm formation in squid-colonizing *V.***
685 ***fischeri***. Phylogenetic tree is simplified from Figure 1, and illustrates key features of squid
686 symbionts in the three groups. Shown are divergent aspects (RscS, SypE) and conserved
687 regulation (BinK). In all groups, the *syp* exopolysaccharide locus is required for squid
688 colonization.
689
690 **SUPPLEMENTAL FILES**

691

692 **Table S1 (PDF). Primer pairs for construction of the deletion mutants**. Detailed

693 oligonucleotide and construction details for deletions and the MJM1100 sypE(ntG33Δ) and

694 MJM1130 *sypE*(*nt33*::*G*) strains.

695

696 **File S1 (PDF). Sequence of the synthetic dsDNA, gBlock_erm.** The sequence is provided in

697 FASTA format printed as PDF.

698

699

700 **Table 1. Bacterial strains.**

Strain	**Genotype**	**Source/Reference**
V. fischeri		
MJM1059	MJ11	(25, 53)
MJM1100	ES114	(54)
MJM1104	ES114 (MJM1100) / pKV69	This study
MJM1106	ES114 (MJM1100) / pKG11	This study
MJM1109	MJ11 (MJM1059) / pKV69	This study
MJM1111	MJ11 (MJM1059) / pKG11	This study
MJM1114	MJ12	(53)
MJM1115	CG101	(25)

MJM1117	ES213	(55)
MJM1119	EM18	(25, 53)
MJM1120	EM24	(53, 56)
MJM1121	EM30	(53)
MJM1122	WH1	(57)
MJM1125	SR5	(24)
MJM1126	SA1	(24)
MJM1127	KB1A97	(29)
MJM1128	KB2B1	(29)
MJM1129	KB5A1	(29)
MJM1130	MB11B1	(29)
MJM1136	EM17	(56)
MJM1147	*mjapo*.6.1	(22)
MJM1149	*mjapo*.7.1	(22)
MJM1151	*mjapo*.8.1	(22)
MJM1153	*mjapo*.9.1	(22)
MJM1219	*mjapo*.8.1 / pKV69	This study

MJM1221	*mjapo*.8.1 / pKG11	This study
MJM1238	MJ12 (MJM1114) / pKV69	This study
MJM1239	MJ12 (MJM1114) / pKG11	This study
MJM1240	SR5 (MJM1125) / pKV69	This study
MJM1241	SR5 (MJM1125) / pKG11	This study
MJM1242	SA1 (MJM1126) / pKV69	This study
MJM1243	SA1 (MJM1126) / pKG11	This study
MJM1244	MB11B1 (MJM1130) / pKV69	This study
MJM1245	MB11B1 (MJM1130) / pKG11	This study
MJM1246	EM17 (MJM1136) / pKV69	This study
MJM1247	EM17 (MJM1136) / pKG11	This study
MJM1254	KB1A97 (MJM1127) / pKV69	This study
MJM1255	KB1A97 (MJM1127) / pKG11	This study
MJM1256	KB2B1 (MJM1128) / pKV69	This study
MJM1257	KB2B1 (MJM1128) / pKG11	This study
MJM1258	KB5A1 (MJM1129) / pKV69	This study
MJM1259	KB5A1 (MJM1129) / pKG11	This study

MJM1260	ES213 (MJM1117) / pKV69	This study
MJM1261	ES213 (MJM1117) / pKG11	This study
MJM1266	EM18 (MJM1119) / pKV69	This study
MJM1267	EM18 (MJM1119) / pKG11	This study
MJM1268	EM24 (MJM1120) / pKV69	This study
MJM1269	EM24 (MJM1120) / pKG11	This study
MJM1270	EM30 (MJM1121) / pKV69	This study
MJM1271	EM30 (MJM1121) / pKG11	This study
MJM1272	*mjapo*.6.1 (MJM1147) / pKV69	This study
MJM1273	*mjapo*.6.1 (MJM1147) / pKG11	This study
MJM1274	*mjapo*.7.1 (MJM1149) / pKV69	This study
MJM1275	*mjapo*.7.1 (MJM1149) / pKG11	This study
MJM1276	*mjapo*.9.1 (MJM1151) / pKV69	This study
MJM1277	*mjapo*.9.1 (MJM1151) / pKG11	This study
MJM1278	CG101 (MJM1115) / pKV69	This study
MJM1279	CG101 (MJM1115) / pKG11	This study
MJM1280	WH1 (MJM1122) / pKV69	This study

MJM1281	WH1 (MJM1122) / pKG11	This study
MJM1782	ES114 (MJM1100) pVSV104	(18)
MJM2114	MB15A4	(29)
MJM2226	ES114 (MJM1100) / pMJM33	This study
MJM2251	ES114 (MJM1100) Δ*binK*	(18)
MJM2386	ES114 (MJM1100) / pBinK	This study
MJM2997	MB11B1 (MJM1130) / pVSV104	This study
MJM2998	MB11B1 (MJM1130) / pBinK	This study
MJM2999	ES213 (MJM1117) / pVSV104	This study
MJM3000	ES213 (MJM1117) / pBinK	This study
MJM3010	ES114 (MJM1100) Δ*rscS*	This study
MJM3017	ES213 (MJM1117) Δ*rscS*	This study
MJM3042	MB15A4 (MJM2114) Δ*rscS*	This study
MJM3046	MB11B1 (MJM1130) Δ*rscS*	This study
MJM3062	ES114 (MJM1100) Δ*syp*	This study
MJM3065	MB11B1 (MJM1130) Δ*syp*	This study
MJM3068	ES213 (MJM1117) Δ*syp*	This study

MJM3071	MB15A4 (MJM2114) Δ*syp*	This study
MJM3084	MB11B1 (MJM1130) Δ*binK*	This study
MJM3354	ES114 (MJM1100) *sypE*(ntG33Δ)	This study
MJM3364	ES114 (MJM1100) *sypE*(ntG33Δ) / pKV69	This study
MJM3365	ES114 (MJM1100) *sypE*(ntG33Δ) / pEAH73	This study
MJM3370	MB11B1 (MJM1130) / pKV69	This study
MJM3371	MB11B1 (MJM1130) / pEAH73	This study
MJM3394	ES114 (MJM1100) Δ*rscS* *sypE*(ntG33Δ)	This study
MJM3397	MB11B1 (MJM1130) *sypE*(nt33::G)	This study
MJM3398	MB11B1 (MJM1130) *sypE*(nt33::G) / pKV69	This study
MJM3399	MB11B1 (MJM1130) *sypE*(nt33::G) / pEAH73	This study
MJM3410	MB11B1 (MJM1130) Δ*sypE*	This study
MJM3411	MB11B1 (MJM1130) Δ*sypE* / pKV69	This study
MJM3412	MB11B1 (MJM1130) Δ*sypE* / pEAH73	This study
MJM3417	ES114 (MJM1100) Δ*sypE*	This study
MJM3418	ES114 (MJM1100) Δ*sypE* / pKV69	This study
MJM3419	ES114 (MJM1100) Δ*sypE* / pEAH73	This study

MJM3423	ES114 (MJM1100) Δ*rscS* Δ*sypE*	This study
MJM3455	ES114 (MJM1100) / pEAH73	This study
MJM3501	SR5 (MJM1125) Δ*syp*	This study
MJM3751	SR5 (MJM1125) ΔbinK::*erm*	This study
E. coli		
MJM534	CC118 λpir / pEVS104	(58)
MJM537	DH5α λpir	Lab stock
MJM570	DH5α / pEVS79	(58)
MJM580	DH5α λpir / pVSV104	(59)
MJM581	DH5α / pKV69	(60)
MJM583	DH5α / pKG11	(15)
MJM639	XL1-Blue / pMJM33	This study
MJM658	BW23474 / pEVS107	(61)
MJM2384	DH5α λpir / pBinK	(18)
MJM2540	KV5264 / pEAH73	(39)
MJM3008	DH5α / pEVS79-Δ*rscS*[MJM1100]	This study
MJM3014	DH5α λpir / pEVS79-Δ*rscS*[MJM1117]	This study

MJM3039	DH5α λpir / pEVS79-Δ*rscS*[MJM2114]	This study
MJM3043	DH5α λpir / pEVS79-Δ*rscS*[MJM1130]	This study
MJM3060	NEB5α / pEVS79-Δ*syp*[MJM1100]	This study
MJM3063	NEB5α / pEVS79-Δ*syp*[MJM1130]	This study
MJM3066	DH5α λpir / pEVS79-Δ*syp[*MJM1117]	This study
MJM3069	DH5α λpir / pEVS79-Δ*syp*[MJM2114]	This study
MJM3082	NEB5α / pEVS79-Δ*binK*[MJM1130]	This study
MJM3287	NEB5α / pHB1	This study
MJM3338	DH5α λpir / pEVS107-*sypE*[MJM1130](nt33::G)	This study
MJM3340	DH5α λpir / pEVS107-*sypE*[MJM1100](ntG33Δ)	This study
MJM3351	NEB5α / pEVS79-*sypE*[MJM1130](nt33::G)	This study
MJM3352	NEB5α / pEVS79-*sypE*[MJM1100](ntG33Δ)	This study
MJM3409	NEB5α / pEVS79-Δ*sypE*[MJM1130]	This study
MJM3416	NEB5α / pEVS79-Δ*sypE*[MJM1100]	This study

701

702 **Table 2. Plasmids.**

Plasmid	**Relevant genotype**	**Source/Reference**
pEVS79	Vector backbone (Cam^R) for deletion	(58)

	construction	
pKV69	Vector backbone (Cam^R/Tet^R)	(60)
pKG11	pKV69 carrying *rscS1*	(15)
pMJM33	pKG11 *rscS1*(ntA1141::Δ)	This study
pEVS104	Conjugation helper plasmid (Kan^R)	(58)
pEVS107	Mini-Tn7 mobilizable vector (Erm^R/Kan^R)	(61)
pEAH73	pKV69 carrying *sypG* from ES114	(39)
pVSV104	Complementation vector (Kan^R)	(59)
pBinK	pVSV104 carrying *binK* from MJM1100	(18)
pHB1	pUC19 FRT-*erm*-FRT	This study
pEVS79-Δ*rscS*[MJM1100]	pEVS79 carrying 1.6 kb US/1.6 kb DS of *rscS* from MJM1100	This study
pEVS79-Δ*rscS*[MJM1117]	pEVS79 carrying 1.6 kb US/1.6 kb DS of *rscS* from MJM1117	This study
pEVS79-Δ*rscS*[MJM2114]	pEVS79 carrying 1.6 kb US/1.6 kb DS of *rscS* from MJM2114	This study
DH5α λpir / pEVS79-Δ*rscS*[MJM1130]	pEVS79 carrying 1.6 kb US/1.6 kb DS of *rscS* from MJM1130	This study
pEVS79-Δ*syp*[MJM1100]	pEVS79 carrying 1.6 kb US of *sypA*/1.6 kb DS of *sypR* from MJM1100	This study
pEVS79-Δ*syp*[MJM1130]	pEVS79 carrying 1.6 kb US of *sypA*/1.6 kb DS of *sypR* from MJM1130	This study
pEVS79-Δ*syp[*MJM1117]	pEVS79 carrying 1.6 kb US of *sypA*/1.6 kb DS of *sypR* from MJM1117	This study

pEVS79-Δ*syp*[MJM2114]	pEVS79 carrying 1.6 kb US of *sypA*/1.6 kb DS of *sypR* from MJM2114	This study
pEVS79-Δ*binK*[MJM1130]	pEVS79 carrying 1.6 kb US/1.6 kb DS of *binK* from MJM1130	This study
pEVS107-*sypE*[MJM1130](nt33::G)	pEVS107 carrying the *sypE*(nt33::G) allele from MJM1130	This study
pEVS107-*sypE*[MJM1100](ntG33Δ)	pEVS107 carrying the *sypE*(ntG33Δ) allele from MJM1100	This study
pEVS79-*sypE*[MJM1130](nt33::G)	pEVS79 carrying the *sypE*(nt33::G) allele from MJM1130	This study
pEVS79-*sypE*[MJM1100](ntG33Δ)	pEVS79 carrying the *sypE*(ntG33Δ) allele from MJM1100	This study
pEVS79-Δ*sypE*[MJM1130]	pEVS79 carrying 1.6 kb US/1.6 kb DS of *sypE* from MJM1130	This study
pEVS79-Δ*sypE*[MJM1100]	pEVS79 carrying 1.6 kb US/1.6 kb DS of *sypE* from MJM1100	This study

703

704

705 **Table 3. DNA oligonucleotides for PCR amplification and sequencing.**

Primer name	**Sequence (5' to 3')**
DAT_015F	ACCAAGAAGCAGTACGACGATTAT
ES114_DS_ver	GGATGTTTTAGATGTTGCGG
ES114_indel_for	TTACTTTTTTCAGATACAAAGCCC
ES114_indel_rev	GTTGTTCTGATAGTGCGTGA
ES114_US_ver	ATCAACTCAAGAAACTCCCC

for_ver_sypE	CCGGCTCAAACTATTGCAG
Gib_ES114_binK_DS_for	attaatcgatGCGTATACATAAATAATGATTCATATATAC
Gib_ES114_binK_DS_rev	gcaggaattcgatatcaagcTTTCAATACTGTGTTTTTATGC
Gib_ES114_binK_US_for	gaggtcgacggtatcgataaGAGCCTTTTAAATCCCCTAAC
Gib_ES114_binK_US_rev	atgtatacgcATCGATTAATGACATATTATTATTCATAAAAAAC
Gib_ES114_rscS_DS_for	taatgcaatgGAGAAGTATGAAACACAATAAAC
Gib_ES114_rscS_DS_rev	gcaggaattcgatatcaagcAAAAATACATTGTTGCACTTG
Gib_ES114_rscS_US_for	gaggtcgacggtatcgataaGACGTCTAAAACTGAATCG
Gib_ES114_rscS_US_rev	catacttctcCATTGCATTAGCTCCTATAAAATAG
Gib_ES114_syp_DS_for	gcttattatgATATTTGCTCGAGGCCAATAAAAAC
Gib_ES114_syp_DS_rev	gcaggaattcgatatcaagcTGGTGAATGTAGGATCCAC
Gib_ES114_syp_US_for	gaggtcgacggtatcgataaCAACCGTAGCGCCAAATG
Gib_ES114_syp_US_rev	gagcaaatatCATAATAAGCTCCTAGGGAATAATC
Gib_ES114_sypE_C_for	cagatacaaaCCCACATCACTAGAGTCG
Gib_ES114_sypE_C_rev	ctagtggccaggtacctcgaAATTAAGCTTCCATCTTCAC
Gib_ES114_sypE_DS_for	tgtaatcatgCTGTTAATTGAGAATCAATAAAAAG
Gib_ES114_sypE_DS_rev	caactctttttccgaaggtaTTGAGTAACCGGCATAATTTAG

Gib_ES114_sypE_N_for	tagagggccctaggcgcgccTGTTTCACAACTCAATACC
Gib_ES114_sypE_N_rev	gtgatgtgggTTTGTATCTGAAAAAAGTAAAGTAG
Gib_ES114_sypE_US_for	gaggtcgacggtatcgataaTGGTCAGATGAAATGTCATTTTTAG
Gib_ES114_sypE_US_rev	caattaacagCATGATTACACCACTGTTG
Gib_ES213_rscS_US_rev	catacttctcCATTGTATTAGCTCCTATAAAATAG
Gib_MB11B1_syp_DS_for	gcttattatgATATTTGCTCGAGGTCAATAAAAG
Gib_MB11B1_syp_US_for	gaggtcgacggtatcgataaGCACACTGATAACTAAATTATTAC
Gib_MB11B1_syp_US_rev	gagcaaatatCATAATAAGCTCCTAGGG
Gib_MB11B1_sypE_C_for	cagatacaaaGCCAACATCACTAGAATC
Gib_MB11B1_sypE_C_rev	ctagtggccaggtacctcgaTCAACAATTAAGCTTCCATC
Gib_MB11B1_sypE_DS_for	cagtggtatgCTGTTAATTGAAAACCAATAGC
Gib_MB11B1_sypE_DS_rev	gcaggaattcgatatcaagcATTTAGGATGTTTTTAATAACAATTTG
Gib_MB11B1_sypE_N_for	tagagggccctaggcgcgccAGTTTCACAACTCAATACTAATAATATTC
Gib_MB11B1_sypE_N_rev	tgatgttggcTTTGTATCTGAAAAAAGCAAAATAG
Gib_MB11B1_sypE_US_for	gaggtcgacggtatcgataaGAATGGTCAGATGAAATGTC
Gib_MB11B1_sypE_US_rev	caattaacagCATACCACTGTTGATAAAAATC
Gib_pEVS79_ES_sypE_for	gaggtcgacggtatcgataaTGTTTCACAACTCAATACC

Gib_pEVS79_ES_sypE_rev	gcaggaattcgatatcaagcAATTAAGCTTCCATCTTCAC
Gib_pEVS79_MB_sypE_for	gaggtcgacggtatcgataaAGTTTCACAACTCAATACTAATAATATTC
Gib_pEVS79_MB_sypE_rev	gcaggaattcgatatcaagcTCAACAATTAAGCTTCCATC
Gib_SR5_syp_DS_for	gcttattatgATATTTGCTCGAGGACAATAAAAAG
Gib_SR5_syp_DS_rev	gcaggaattcgatatcaagcTGGTGAGTGTAGAATCCATTC
Gib_SR5_syp_US_for	gaggtcgacggtatcgataaAACCGTAGCGCCAAATGG
Gib_SR5_syp_US_rev	gagcaaatatCATAATAAGCTCCTAGGGAATAATCC
HB8	ACAAAATTTTAAGATACTGCACTATCAACACACTCTTAAG
HB9	GGGAGGAAATAATCTAGAATGCGAGAGTAGG
HB23	TTGGAGAGCCAGCTGCGTTCGCTAA
HB39	TAGGAAGCTTACGAGACGAGCTTCTTATATATGCTTCGCCAGGAAGTTCCTATTCTCTAGAAAGTATAGGAACTTCCTTAGAAGCAAACTTAAGAGTGTG
HB41	CGATCTTGTGGGTAGAGACATCCAGGTCAAGTCCAGCCCCGCTCTAGTTTGGGAATCAAGTGCATGAGCGCTGAAG
HB42	ACGAGACGAGCTTCTTATATATGCTTCGCCAG
HB146	CGATCTTGTGGGTAGAGACATC
binK-F1	GAAATTACCATGGAGCCAACAGCAAGAC
binK-R1-LUH	ctggcgaagcatatataagaagctcgtctcgtCATAAAAAACCTAGCGCTTTATTTGTAGATATAATTATTAACTATAATCGC

binK-F2-RUH	gacttgacctggatgtctctacccacaagatcgCGCTCATTGTATCTATAGAGTATGTACTGAGTTACG
binK-R2	GGCATCATTATGGCAACCATTAAAGACG
binK-FO	CCGTTAATACTGGATTATTCGCTTGAATTTGAACG
KMB_036	CCACAATAGCAGAATACAAATTCGCTG
KMB_037	CTCAAAATGACAGTCAGAGTATCGTAGGC
JFB_287	ATGGAGTTTCTACGTCAACCAGAA
JFB_287_MB11B1	ATGGAGTTTTTACGTCAACCAGAG
JFB_288	TGTTATAACGATTACATGGCAGCG
JFB_365	GGAAAGAGAATGATTAAG
M13for	GTAAAACGACGGCCAG
M13rev	CAGGAAACAGCTATGAC
MB11B1_indel_for	GCTTTTTTCAGATACAAAGCCA
MB11B1_indel_rev	ATACCTGATGGAAACGACCT
MJM-154F	TAAAAAGGGAATTAATCCGC
MJM-306R	AACTCTAACCAAGAAGCA
pEVS107_3837	GGCGCGCCTAGGGCCCTC
pEVS107_3838	TCGAGGTACCTGGCCACTAG

pEVS79_for_691	GCTTGATATCGAATTCCTG
pEVS79_rev_690	TTATCGATACCGTCGACC
rev_ver_sypE	TTCACCATGAGTGCCAAATC
rscS_del1F	CTTATCTTCTAGTTCTTTTTTTTAGTGATGTCTCTTTC TACGGC
rscS_del1R	GCCGTAGAAAGAGACATCACTAAAAAAAAGAACTAG AAGATAAG
rscS_ver_1	GTAATTCAGTAATGCTACC
rscS_ver_2	GTCGCACCGTCAGGTATA
rscS_ver_3	AAGAAATTATTCGCTACC
rscS_ver_4	AGTTAGTAGGCCATTACG
SR5_syp_ver_for	TAGGCGTATCAAAAACCACCT
SR5_syp_ver_rev	TCAGGAATGTCGATGGCAG
Syp_ver_DS_rev	ATCGAGCATATTTTGCCAATC
Syp_ver_US_for	ACCTATCAACTCTTAAGTCGATTC
syp4F	TGAGGATCCCATCGTGCCATA
syp4R	AGCTCCTTTGCAATGTTTGCTT
syp5F	TATTAGGCCGTTTCCACCAGG
syp5F-B	TATTAGGTCGTTTCCATCAGG

sypA_out	AACAGGAATTGCGTTTTCAA
US_syp_flank_for	ACCACTGTGATAACTTGCAC
US_syp_flank_rev	ATGAGGCATAACCTGTTCCA

706 For Gibson assembly primers, capital letters indicate homology to the template. All primers were
707 designed for this study except MJM-154F, MJM-306R (22); JFB_287, JFB_288, and JFB_365
708 (18); and M13 for, M13 rev.
709

710 **ACKNOWLEDGMENTS**

711

712 The authors thank Elizabeth Bacon, Jacklyn Duple, Cheeneng Moua, Lynn Naughton, Olivia
713 Sauls, and Denise Tarnowski for assistance with experiments.
714

715 **FUNDING INFORMATION**

716

717 This work was funded by NIH grants R35GM119627 (to M.J.M.) and R21AI117262 (M.J.M.) and
718 NSF grant IOS-1757297 (M.J.M.). Support for trainees was provided on NIGMS grants
719 T32GM008061 (J.F.B.) and T32GM008349 (K.M.B.). This work was funded by the Chicago
720 Biomedical Consortium with support from the Searle Funds at The Chicago Community Trust
721 (supporting E.R.R.).
722

723 **REFERENCES**

724 1. Long SR. 1996. *Rhizobium* symbiosis: nod factors in perspective. Plant Cell 8:1885–1898.

725 2. Roche P, Maillet F, Plazanet C, Debellé F, Ferro M, Truchet G, Promé JC, Dénarié J. 1996.

726 The common *nodABC* genes of *Rhizobium meliloti* are host-range determinants. Proc Natl
727 Acad Sci U S A 93:15305–15310.

728 3. Costello EK, Lauber CL, Hamady M, Fierer N, Gordon JI, Knight R. 2009. Bacterial
729 community variation in human body habitats across space and time. Science 326:1694–
730 1697.

731 4. Grice EA, Kong HH, Conlan S, Deming CB, Davis J, Young AC, NISC Comparative
732 Sequencing Program, Bouffard GG, Blakesley RW, Murray PR, Green ED, Turner ML,
733 Segre JA. 2009. Topographical and temporal diversity of the human skin microbiome.
734 Science 324:1190–1192.

735 5. Mark Welch JL, Rossetti BJ, Rieken CW, Dewhirst FE, Borisy GG. 2016. Biogeography of a
736 human oral microbiome at the micron scale. Proc Natl Acad Sci U S A 113:E791–E800.

737 6. Ruby EG. 2008. Symbiotic conversations are revealed under genetic interrogation. Nat Rev
738 Microbiol 6:752–762.

739 7. Nyholm SV, McFall-Ngai MJ. 2004. The winnowing: establishing the squid-vibrio symbiosis.
740 Nat Rev Microbiol 2:632–642.

741 8. Visick KL, Ruby EG. 2006. *Vibrio fischeri* and its host: it takes two to tango. Curr Opin
742 Microbiol 9:632–638.

743 9. Mandel MJ, Schaefer AL, Brennan CA, Heath-Heckman EAC, Deloney-Marino CR, McFall-
744 Ngai MJ, Ruby EG. 2012. Squid-derived chitin oligosaccharides are a chemotactic signal
745 during colonization by *Vibrio fischeri*. Appl Environ Microbiol 78:4620–4626.

746 10. Jones BW, Nishiguchi MK. 2004. Counterillumination in the Hawaiian bobtail squid,
747 *Euprymna scolopes* Berry (Mollusca: Cephalopoda). Mar Biol 144:1151–1155.

748 11. Ruby EG, McFall-Ngai MJ. 1992. A squid that glows in the night: development of an animal-
749 bacterial mutualism. J Bacteriol 174:4865–4870.

750 12. Wier AM, Nyholm SV, Mandel MJ, Massengo-Tiassé RP, Schaefer AL, Koroleva I, Splinter-
751 Bondurant S, Brown B, Manzella L, Snir E, Almabrazi H, Scheetz TE, Bonaldo M de F,
752 Casavant TL, Soares MB, Cronan JE, Reed JL, Ruby EG, McFall-Ngai MJ. 2010.
753 Transcriptional patterns in both host and bacterium underlie a daily rhythm of anatomical
754 and metabolic change in a beneficial symbiosis. Proc Natl Acad Sci U S A 107:2259–2264.

755 13. Visick KL. 2009. An intricate network of regulators controls biofilm formation and
756 colonization by *Vibrio fischeri*. Mol Microbiol 74:782–789.

757 14. Yip ES, Grublesky BT, Hussa EA, Visick KL. 2005. A novel, conserved cluster of genes
758 promotes symbiotic colonization and σ^{54}-dependent biofilm formation by *Vibrio fischeri*. Mol
759 Microbiol 57:1485–1498.

760 15. Yip ES, Geszvain K, DeLoney-Marino CR, Visick KL. 2006. The symbiosis regulator RscS
761 controls the *syp* gene locus, biofilm formation and symbiotic aggregation by *Vibrio fischeri*.
762 Mol Microbiol 62:1586–1600.

763 16. Shibata S, Yip ES, Quirke KP, Ondrey JM, Visick KL. 2012. Roles of the Structural
764 Symbiosis Polysaccharide (*syp*) Genes in Host Colonization, Biofilm Formation, and
765 Polysaccharide Biosynthesis in *Vibrio fischeri*. J Bacteriol 194:6736–6747.

766 17. Morris AR, Visick KL. 2013. The response regulator SypE controls biofilm formation and
767 colonization through phosphorylation of the syp-encoded regulator SypA in *Vibrio fischeri*.
768 Mol Microbiol 87:509–525.

769 18. Brooks JF 2nd, Mandel MJ. 2016. The Histidine Kinase BinK Is a Negative Regulator of
770 Biofilm Formation and Squid Colonization. J Bacteriol 198:2596–2607.

771 19. Tischler AH, Lie L, Thompson CM, Visick KL. 2018. Discovery of Calcium as a Biofilm-
772 Promoting Signal for Vibrio fischeri Reveals New Phenotypes and Underlying Regulatory
773 Complexity. J Bacteriol 200:e00016–18.

774 20. Pankey MS, Foxall RL, Ster IM, Perry LA, Schuster BM, Donner RA, Coyle M, Cooper VS,
775 Whistler CA. 2017. Host-selected mutations converging on a global regulator drive an
776 adaptive leap towards symbiosis in bacteria. Elife 6:e24414.

777 21. Thompson CM, Tischler AH, Tarnowski DA, Mandel MJ, Visick KL. 2018. Nitric oxide
778 inhibits biofilm formation by *Vibrio fischeri* via the nitric oxide-sensor HnoX. Mol Microbiol
779 doi:10.1111/mmi.14147.

780 22. Mandel MJ, Wollenberg MS, Stabb EV, Visick KL, Ruby EG. 2009. A single regulatory gene
781 is sufficient to alter bacterial host range. Nature 458:215–218.

782 23. Nyholm SV, Nishiguchi MK. 2008. The evolutionary ecology of a sepiolid squid-vibrio
783 association: from cell to environment. Vie Milieu Paris 58:175–184.

784 24. Fidopiastis PM, von Boletzky S, Ruby EG. 1998. A new niche for *Vibrio logei*, the
785 predominant light organ symbiont of squids in the genus *Sepiola*. J Bacteriol 180:59–64.

786 25. Ruby EG, Lee KH. 1998. The *Vibrio fischeri-Euprymna scolopes* Light Organ Association:
787 Current Ecological Paradigms. Appl Environ Microbiol 64:805–812.

788 26. Mandel MJ. 2010. Models and approaches to dissect host-symbiont specificity. Trends
789 Microbiol 18:504–511.

790 27. Gyllborg MC, Sahl JW, Cronin DC 3rd, Rasko DA, Mandel MJ. 2012. Draft genome
791 sequence of *Vibrio fischeri* SR5, a strain isolated from the light organ of the Mediterranean
792 squid *Sepiola robusta*. J Bacteriol 194:1639.

793 28. Geszvain K, Visick KL. 2008. Multiple factors contribute to keeping levels of the symbiosis
794 regulator RscS low. FEMS Microbiol Lett 285:33–39.

795 29. Wollenberg MS, Ruby EG. 2009. Population structure of *Vibrio fischeri* within the light
796 organs of *Euprymna scolopes* squid from Two Oahu (Hawaii) populations. Appl Environ
797 Microbiol 75:193–202.

798 30. Wollenberg MS, Ruby EG. 2012. Phylogeny and fitness of *Vibrio fischeri* from the light
799 organs of *Euprymna scolopes* in two Oahu, Hawaii populations. ISME J 6:352–362.

800 31. Elliott KT, DiRita VJ. 2008. Characterization of CetA and CetB, a bipartite energy taxis
801 system in *Campylobacter jejuni*. Mol Microbiol 69:1091–1103.

802 32. Antonov I, Coakley A, Atkins JF, Baranov PV, Borodovsky M. 2013. Identification of the
803 nature of reading frame transitions observed in prokaryotic genomes. Nucleic Acids Res
804 41:6514–6530.

805 33. Bongrand C, Koch EJ, Moriano-Gutierrez S, Cordero OX, McFall-Ngai M, Polz MF, Ruby
806 EG. 2016. A genomic comparison of 13 symbiotic *Vibrio fischeri* isolates from the
807 perspective of their host source and colonization behavior. ISME J 10:2907–2917.

808 34. Altschul SF, Madden TL, Schäffer AA, Zhang J, Zhang Z, Miller W, Lipman DJ. 1997.
809 Gapped BLAST and PSI-BLAST: a new generation of protein database search programs.
810 Nucleic Acids Res 25:3389–3402.

811 35. Rusch DB, Rowe-Magnus DA. 2017. Complete Genome Sequence of the Pathogenic
812 *Vibrio vulnificus* Type Strain ATCC 27562. Genome Announc 5:e00907–17.

813 36. Morris AR, Darnell CL, Visick KL. 2011. Inactivation of a novel response regulator is
814 necessary for biofilm formation and host colonization by *Vibrio fischeri*. Mol Microbiol

815 82:114–130.

816 37. Guo Y, Rowe-Magnus DA. 2011. Overlapping and unique contributions of two conserved
817 polysaccharide loci in governing distinct survival phenotypes in Vibrio vulnificus. Environ
818 Microbiol 13:2888–2990.

819 38. Morris AR, Visick KL. 2013. Inhibition of SypG-induced biofilms and host colonization by the
820 negative regulator SypE in *Vibrio fischeri*. PLoS One 8:e60076.

821 39. Hussa EA, Darnell CL, Visick KL. 2008. RscS functions upstream of SypG to control the
822 syp locus and biofilm formation in *Vibrio fischeri*. J Bacteriol 190:4576–4583.

823 40. Koehler S, Gaedeke R, Thompson C, Bongrand C, Visick KL, Ruby E, McFall-Ngai M.
824 2018. The model squid-vibrio symbiosis provides a window into the impact of strain- and
825 species-level differences during the initial stages of symbiont engagement. Environ
826 Microbiol doi:10.1111/1462–2920.14392.

827 41. Ray VA, Visick KL. 2012. LuxU connects quorum sensing to biofilm formation in *Vibrio*
828 *fischeri*. Mol Microbiol 86:954–970.

829 42. Giraud E, Moulin L, Vallenet D, Barbe V, Cytryn E, Avarre J-C, Jaubert M, Simon D,
830 Cartieaux F, Prin Y, Bena G, Hannibal L, Fardoux J, Kojadinovic M, Vuillet L, Lajus A,
831 Cruveiller S, Rouy Z, Mangenot S, Segurens B, Dossat C, Franck WL, Chang W-S,
832 Saunders E, Bruce D, Richardson P, Normand P, Dreyfus B, Pignol D, Stacey G, Emerich
833 D, Verméglio A, Médigue C, Sadowsky M. 2007. Legumes symbioses: absence of Nod
834 genes in photosynthetic bradyrhizobia. Science 316:1307–1312.

835 43. Bonaldi K, Gargani D, Prin Y, Fardoux J, Gully D, Nouwen N, Goormachtig S, Giraud E.
836 2011. Nodulation of *Aeschynomene afraspera* and *A. indica* by photosynthetic
837 *Bradyrhizobium* Sp. strain ORS285: the Nod-dependent versus the Nod-independent

838 symbiotic interaction. Mol Plant Microbe Interact 24:1359–1371.

839 44. Darriba D, Taboada GL, Doallo R, Posada D. 2012. jModelTest 2: more models, new
840 heuristics and parallel computing. Nat Methods 9:772.

841 45. Swofford DL. 2003. PAUP*: Phylogenetic Analysis Using Parsimony (* and Other Methods)
842 4th edn. Sinauer.

843 46. Ronquist F, Teslenko M, van der Mark P, Ayres DL, Darling A, Höhna S, Larget B, Liu L,
844 Suchard MA, Huelsenbeck JP. 2012. MrBayes 3.2: efficient Bayesian phylogenetic
845 inference and model choice across a large model space. Syst Biol 61:539–542.

846 47. Ronquist F, van der Mark P, Huelsenbeck JP. 2009. Bayesian phylogenetic analysis using
847 MrBayes, 2nd edn. Cambridge University Press.

848 48. Visick KL, Hodge-Hanson KM, Tischler AH, Bennett AK, Mastrodomenico V. 2018. Tools
849 for Rapid Genetic Engineering of *Vibrio fischeri*. Appl Environ Microbiol 84:e00850–18.

850 49. Pollack-Berti A, Wollenberg MS, Ruby EG. 2010. Natural transformation of *Vibrio fischeri*
851 requires *tfoX* and *tfoY*. Environ Microbiol 12:2302–2311.

852 50. Baba T, Ara T, Hasegawa M, Takai Y, Okumura Y, Baba M, Datsenko KA, Tomita M,
853 Wanner BL, Mori H. 2006. Construction of *Escherichia coli* K-12 in-frame, single-gene
854 knockout mutants: the Keio collection. Mol Syst Biol 2:2006.0008.

855 51. Naughton LM, Mandel MJ. 2012. Colonization of *Euprymna scolopes* squid by *Vibrio*
856 *fischeri*. J Vis Exp e3758.

857 52. Finn RD, Coggill P, Eberhardt RY, Eddy SR, Mistry J, Mitchell AL, Potter SC, Punta M,
858 Qureshi M, Sangrador-Vegas A, Salazar GA, Tate J, Bateman A. 2016. The Pfam protein
859 families database: towards a more sustainable future. Nucleic Acids Res 44:D279–85.

860 53. Lee K-H. 1994. Ecology of *Vibrio fisheri*: the light organ symbiont of the Hawaiian sepiolid
861 squid *Euprymna scolopes*. University of Southern California.

862 54. Boettcher KJ, Ruby EG. 1990. Depressed light emission by symbiotic *Vibrio fischeri* of the
863 sepiolid squid *Euprymna scolopes*. J Bacteriol 172:3701–3706.

864 55. Boettcher KJ, Ruby EG. 1994. Occurrence of plasmid DNA in the sepiolid squid symbiont
865 *Vibrio fischeri*. Curr Microbiol 29:279–286.

866 56. Nishiguchi MK, Ruby EG, McFall-Ngai MJ. 1998. Competitive dominance among strains of
867 luminous bacteria provides an unusual form of evidence for parallel evolution in Sepiolid
868 squid-vibrio symbioses. Appl Environ Microbiol 64:3209–3213.

869 57. Nishiguchi MK, Nair VS. 2003. Evolution of symbiosis in the Vibrionaceae: a combined
870 approach using molecules and physiology. Int J Syst Evol Microbiol 53:2019–2026.

871 58. Stabb EV, Ruby EG. 2002. RP4-based plasmids for conjugation between *Escherichia coli*
872 and members of the *Vibrionaceae*. Methods Enzymol 358:413–426.

873 59. Dunn AK, Millikan DS, Adin DM, Bose JL, Stabb EV. 2006. New *rfp*- and pES213-derived
874 tools for analyzing symbiotic *Vibrio fischeri* reveal patterns of infection and *lux* expression in
875 situ. Appl Environ Microbiol 72:802–810.

876 60. Visick KL, Skoufos LM. 2001. Two-component sensor required for normal symbiotic
877 colonization of *Euprymna scolopes* by *Vibrio fischeri*. J Bacteriol 183:835–842.

878 61. McCann J, Stabb EV, Millikan DS, Ruby EG. 2003. Population dynamics of *Vibrio fischeri*
879 during infection of *Euprymna scolopes*. Appl Environ Microbiol 69:5928–5934.

880

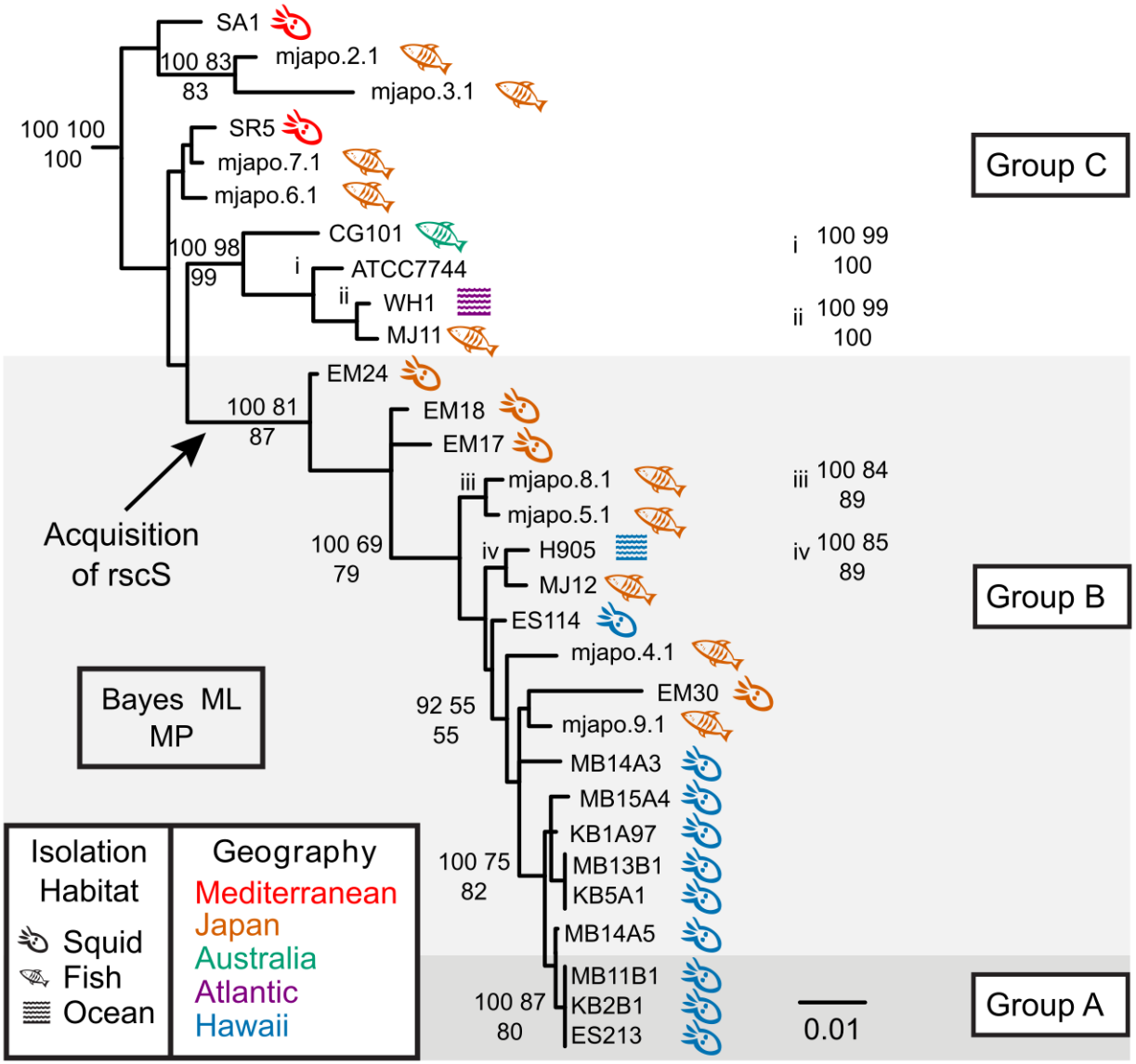
SA1
mjapo.2.1
mjapo.3.1
100 83
83
100 100
100
SR5
mjapo.7.1
mjapo.6.1
Group C
CG101
100 98
99
i
ATCC7744
ii
WH1
MJ11
i 100 99
100
ii 100 99
100
EM24
100 81
87
EM18
EM17
iii
mjapo.8.1
mjapo.5.1
iii 100 84
89
Acquisition
of rscS
100 69
79
iv
H905
MJ12
iv 100 85
89
Group B
ES114
mjapo.4.1
Bayes ML
MP
92 55
55
EM30
mjapo.9.1
MB14A3
MB15A4
KB1A97
100 75
82
MB13B1
KB5A1
MB14A5
MB11B1
100 87
80
KB2B1
ES213
0.01
Group A
Isolation
Habitat
Squid
Fish
Ocean
Geography
Mediterranean
Japan
Australia
Atlantic
Hawaii

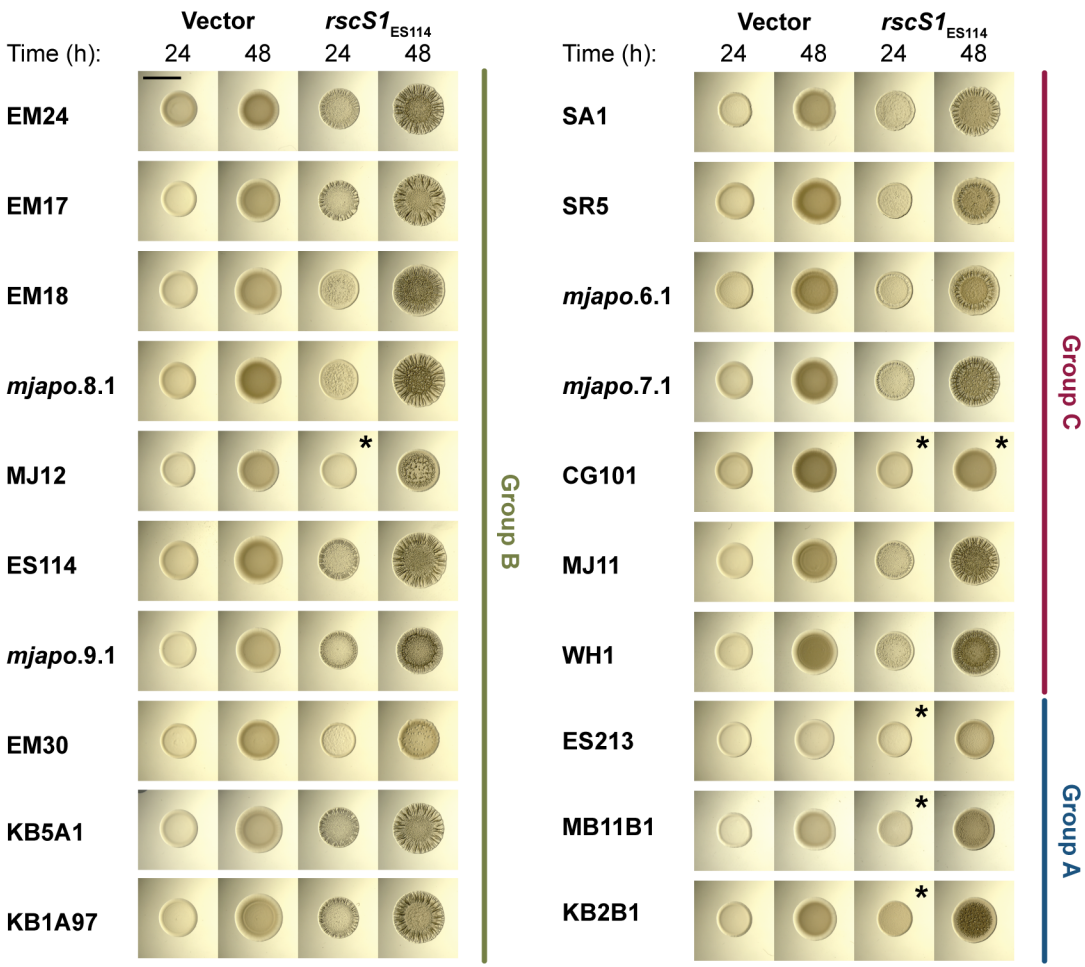
Vector
rscS1ES114
Time (h):
24
48
24
48
EM24
EM17
EM18
mjapo.8.1
MJ12
ES114
mjapo.9.1
EM30
KB5A1
KB1A97
Group B
Vector
rscS1ES114
Time (h):
24
48
24
48
SA1
SR5
mjapo.6.1
mjapo.7.1
CG101
MJ11
WH1
ES213
MB11B1
KB2B1
Group C
Group A

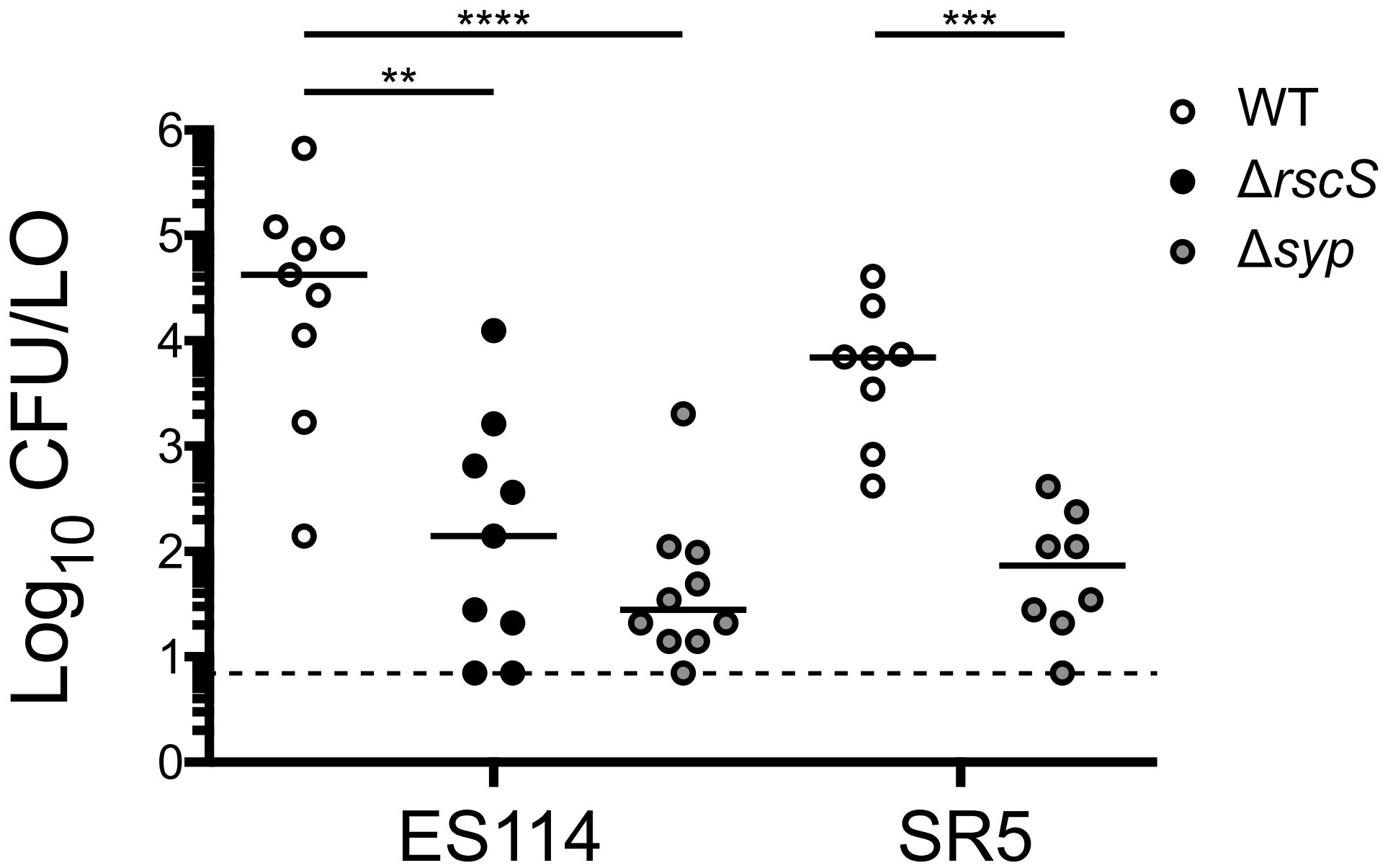
****
***
**
WT
ΔrscS
Δsyp
Log10 CFU/LO
6
5
4
3
2
1
0
ES114
SR5

A

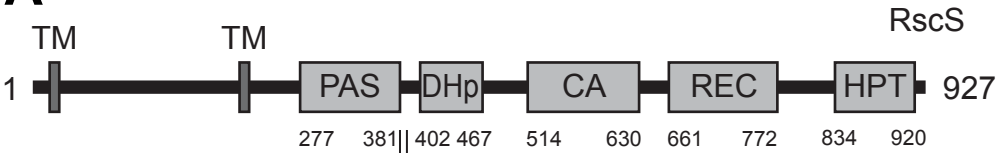


```
EM17     Group B  TACATTGCCGTAGAAAGAGACATCACTAAAAAAAAAGAACTAGAAGATAAGTTAATAAAA
ES114          B  TACATTGCCGTAGAAAGAGACATCACTAAAAAAAAAGAACTAGAAGATAAGTTAATAAAA
MB15A4         B  TACATTGCCGTAGAAAGAGACATCACTAAAAAAAAAGAACTAGAAGATAAGTTAATAAAA
MB11B1   Group A  TACATTGCCGTAGAAAGAGACATCACT-AAAAAAAAGAACTAGAAGATAAGTTAATAAAA
ES213          A  TACATTGCCGTAGAAAGAGACATCACT-AAAAAAAAGAACTAGAAGATAAGTTAATAAAA
KB2B1          A  TACATTGCCGTAGAAAGAGACATCACT-AAAAAAAAGAACTAGAAGATAAGTTAATAAAA
```

B

Vector *rscS1* *rscS1*^{FS}

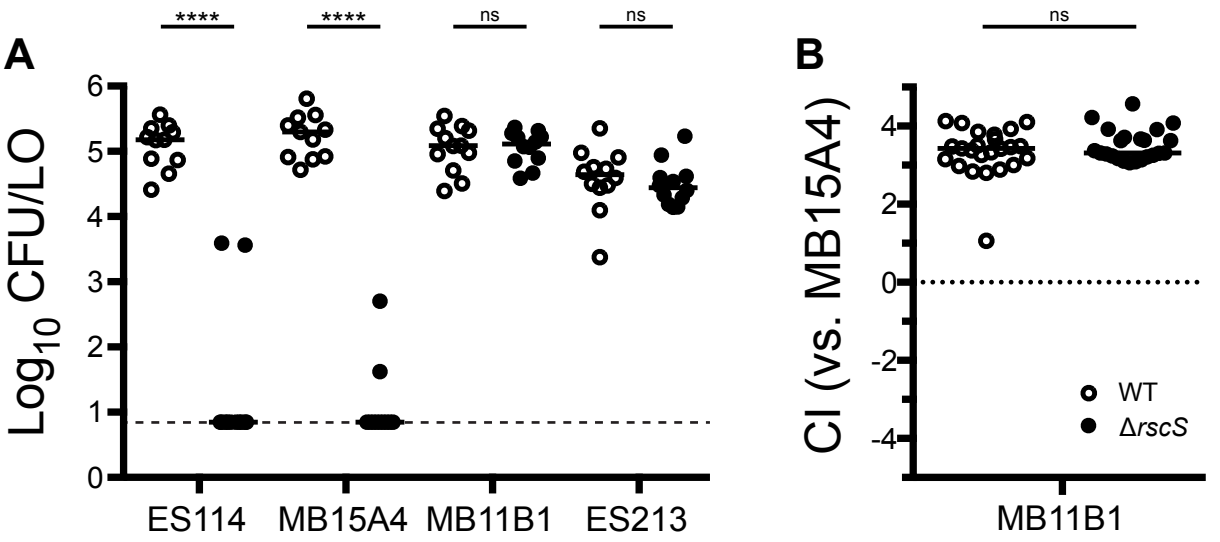
A
****
****
ns
ns
Log10 CFU/LO
6
5
4
3
2
1
0
ES114
MB15A4
MB11B1
ES213
B
ns
CI (vs. MB15A4)
4
2
0
-2
-4
WT
ΔrscS
MB11B1

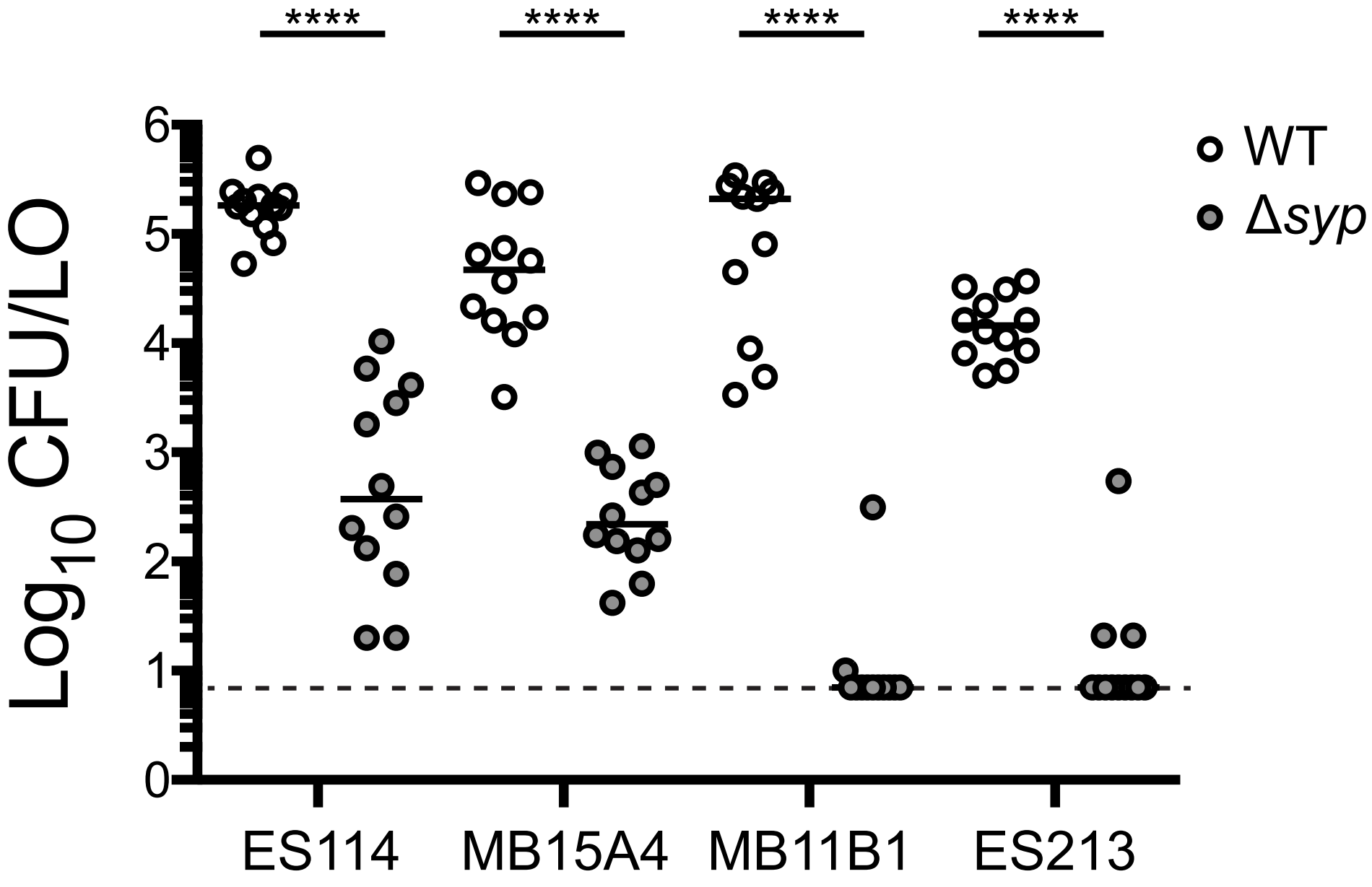
****
****
****
****
Log10 CFU/LO
6
5
4
3
2
1
0
WT
Δsyp
ES114
MB15A4
MB11B1
ES213

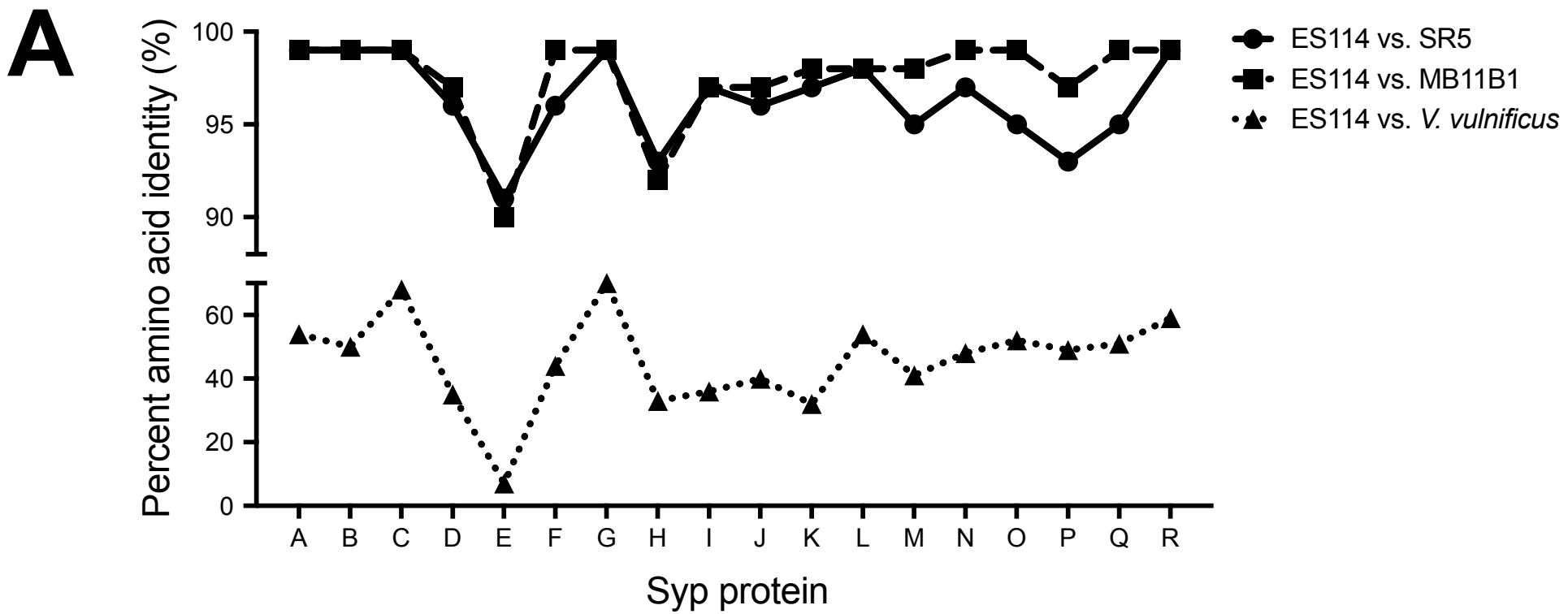
A
Percent amino acid identity (%)
100
95
90
60
40
20
0
A B C D E F G H I J K L M N O P Q R
Syp protein
ES114 vs. SR5
ES114 vs. MB11B1
ES114 vs. V. vulnificus

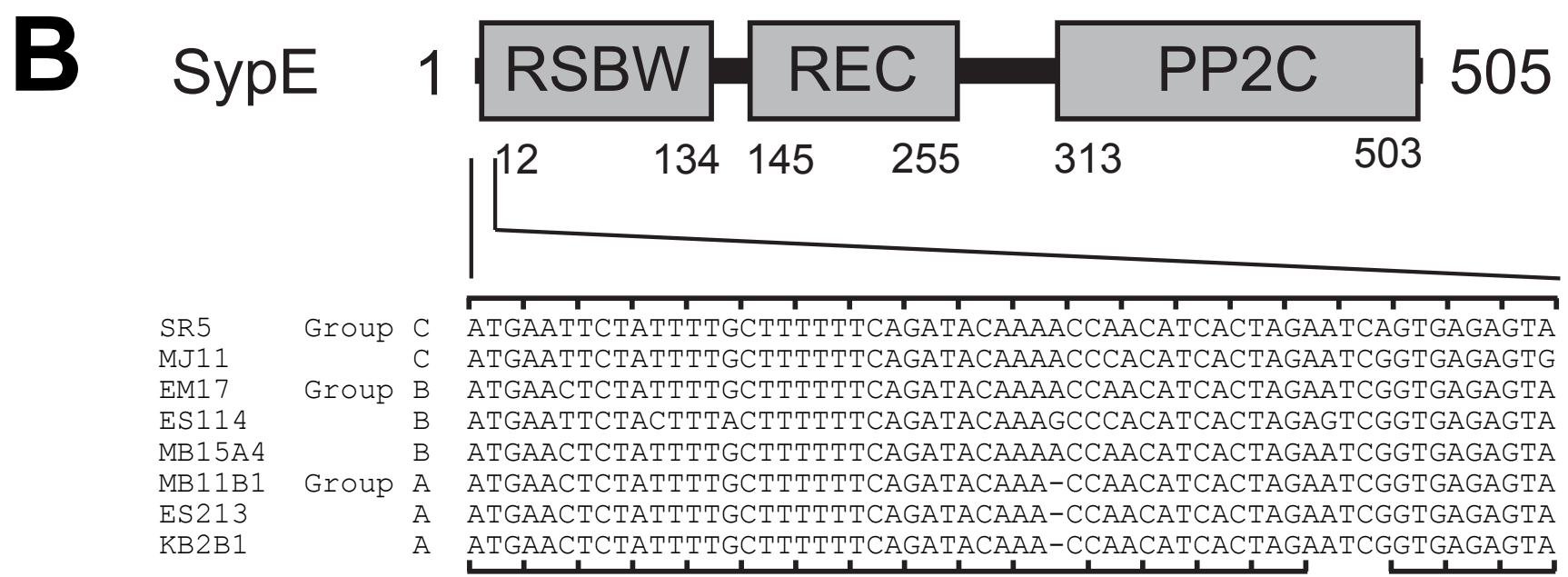
B
SypE
1
RSBW
REC
PP2C
505
12
134
145
255
313
503
SR5 Group C ATGAATTCTATTTTGCTTTTTTCAGATACAAAACCAACATCACTAGAATCAGTGAGAGTA
MJ11 C ATGAATTCTATTTTGCTTTTTTCAGATACAAAACCCACATCACTAGAATCGGTGAGAGTG
EM17 Group B ATGAACTCTATTTTGCTTTTTTCAGATACAAAACCAACATCACTAGAATCGGTGAGAGTA
ES114 B ATGAATTCTACTTTACTTTTTTCAGATACAAAGCCCACATCACTAGAGTCGGTGAGAGTA
MB15A4 B ATGAACTCTATTTTGCTTTTTTCAGATACAAAACCAACATCACTAGAATCGGTGAGAGTA
MB11B1 Group A ATGAACTCTATTTTGCTTTTTTCAGATACAAA-CCAACATCACTAGAATCGGTGAGAGTA
ES213 A ATGAACTCTATTTTGCTTTTTTCAGATACAAA-CCAACATCACTAGAATCGGTGAGAGTA
KB2B1 A ATGAACTCTATTTTGCTTTTTTCAGATACAAA-CCAACATCACTAGAATCGGTGAGAGTA

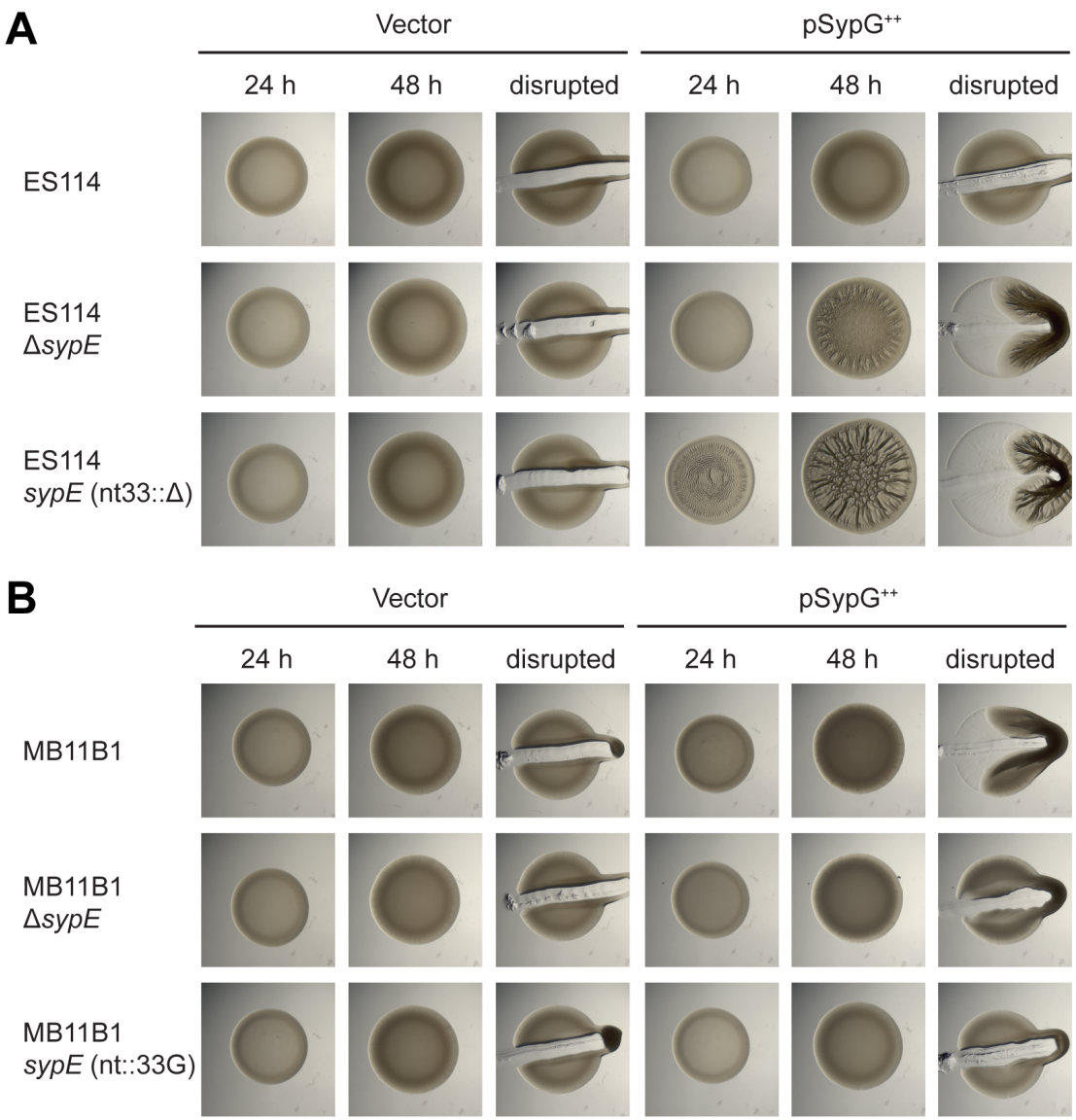
A
Vector
pSypG++
24 h
48 h
disrupted
24 h
48 h
disrupted
ES114
ES114
ΔsypE
ES114
sypE (nt33::Δ)
B
Vector
pSypG++
24 h
48 h
disrupted
24 h
48 h
disrupted
MB11B1
MB11B1
ΔsypE
MB11B1
sypE (nt::33G)

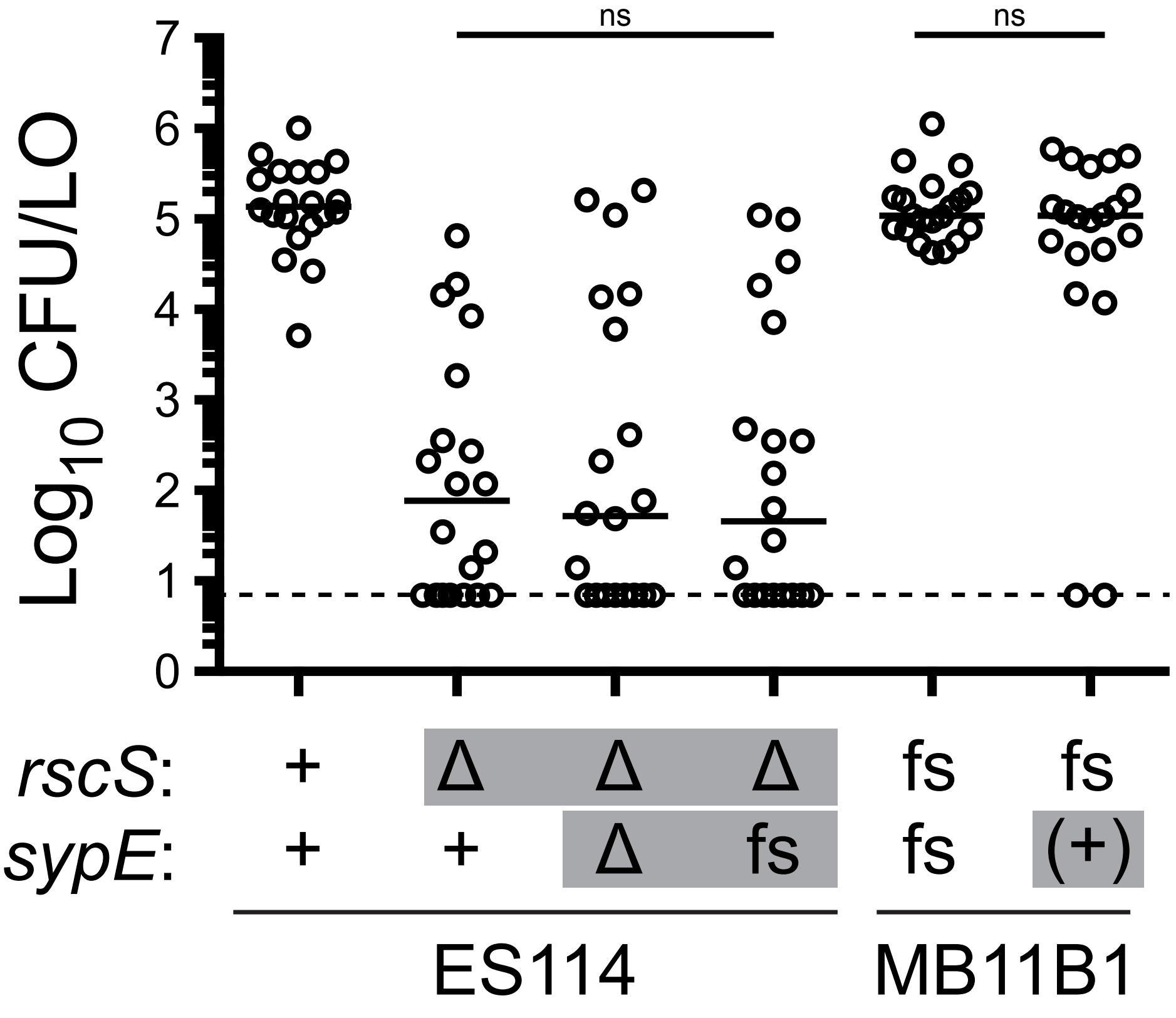
ns
ns
Log10 CFU/LO
7
6
5
4
3
2
1
0
rscS:
+
Δ
Δ
Δ
fs
fs
sypE:
+
+
Δ
fs
fs
(+)
ES114
MB11B1

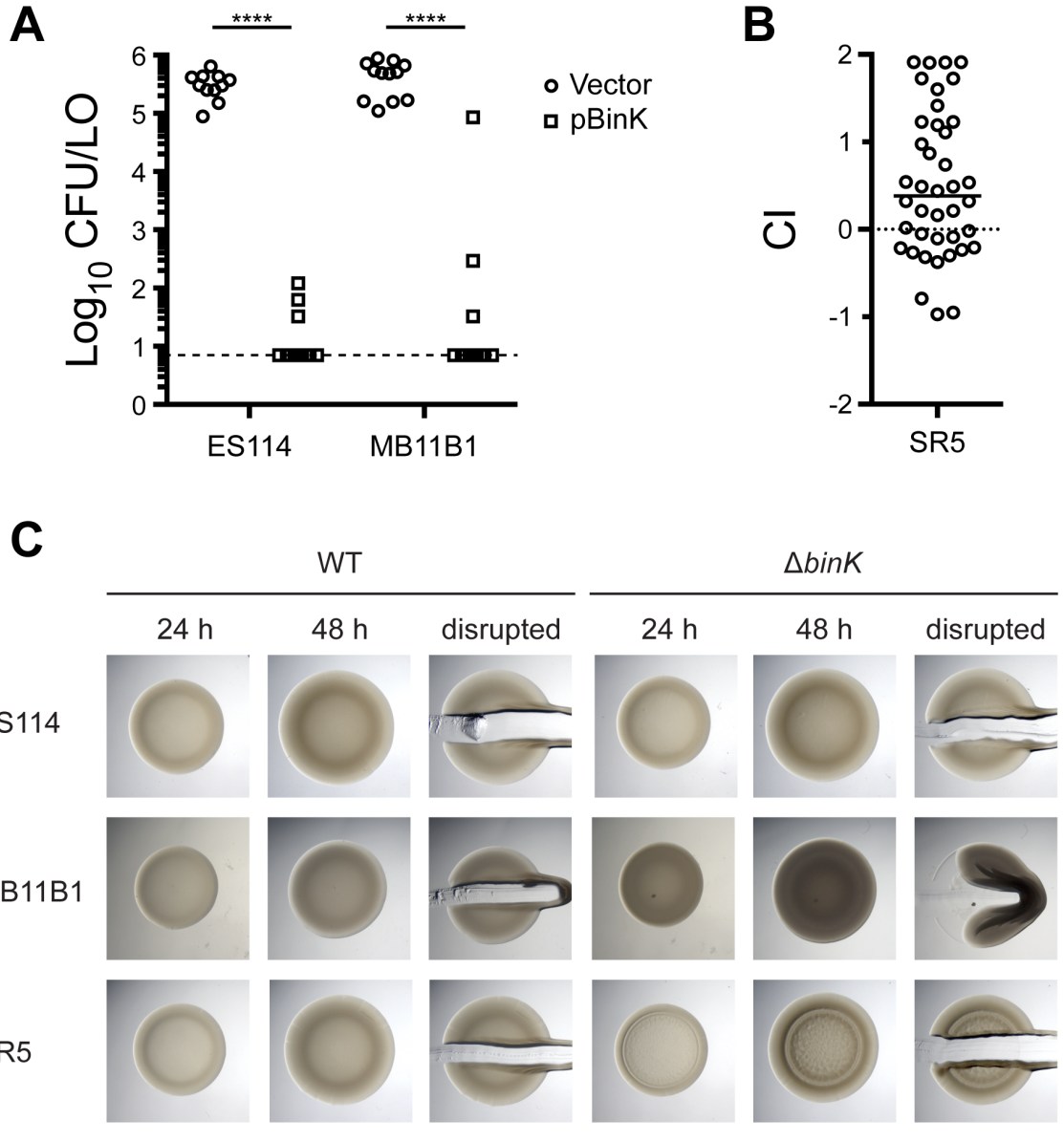
A
****
****
Log10 CFU/LO
6
5
4
3
2
1
0
ES114
MB11B1
Vector
pBinK
B
CI
2
1
0
-1
-2
SR5
C
WT
ΔbinK
24 h
48 h
disrupted
24 h
48 h
disrupted
ES114
MB11B1
SR5

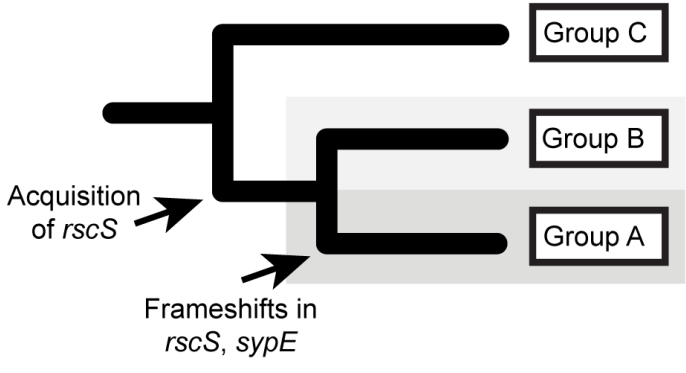

	rscS	**Colonization: RscS**	***sypE***	**Biofilm: BinK**
Group C	No	Not required	Yes	Negative regulator
Group B	Yes	Required	Yes	Negative regulator
Group A	ntA1141Δ	Not required	ntG33Δ	Negative regulator

Table S1. Primers pairs for construction of mutants.

Strain	Note	Forward Primer	Reverse Primer	PCR Product Size	Description of PCR product	E. coli with clone
MJM3010 =		Gib_ES114_rscS_US_for	Gib_ES114_rscS_US_rev	1.6 kb	Gibson assembly cloning of upstream *rscS* region in MJM1100 into pEVS79	**MJM3008**
MJM1100 Δ*rscS* and		Gib_ES114_rscS_DS_for	Gib_ES114_rscS_DS_rev	1.6 kb	Gibson assembly cloning of downstream *rscS* region in MJM1100 into pEVS79	
MJM3394 =		ES114_US_ver	ES114_DS_ver	586 bp	Verification of Δ*rscS* by flanking the upstream/downstream junction	
MJM3354 Δ*rscS*		ES114_US_ver	DAT015F	520 bp	Verification of Δ*rscS*; no product due to one primer binding within *rscS*.	
		Gib_ES114_rscS_US_for	Gib_ES213_rscS_US_rev	1.6 kb	Gibson assembly cloning of upstream *rscS* region in MJM1117 into pEVS79	**MJM3014**
MJM3017 =		Gib_ES114_rscS_DS_for	Gib_ES114_rscS_DS_rev	1.6 kb	Gibson assembly cloning of downstream *rscS* region in MJM1117 into pEVS79	
MJM1117 Δ*rscS*		ES114_US_ver	ES114_DS_ver	586 bp	Verification of Δ*rscS* by flanking the upstream/downstream junction	
		ES114_US_ver	DAT015F	520 bp	Verification of Δ*rscS*; no product due to one primer binding within *rscS*.	
		Gib_ES114_rscS_US_for	Gib_ES114_rscS_US_rev	1.6 kb	Gibson assembly cloning of upstream *rscS* region in MJM1130 into pEVS79	**MJM3043**
MJM3046 =		Gib_ES114_rscS_DS_for	Gib_ES114_rscS_DS_rev	1.6 kb	Gibson assembly cloning of downstream *rscS* region in MJM1130 into pEVS79	
MJM1130 Δ*rscS*		ES114_US_ver	ES114_DS_ver	586 bp	Verification of Δ*rscS* by flanking the upstream/downstream junction	
		ES114_US_ver	DAT015F	520 bp	Verification of Δ*rscS*; no product due to one primer binding within *rscS*	
		Gib_ES114_rscS_US_for	Gib_ES114_rscS_US_rev	1.6 kb	Gibson assembly cloning of upstream *rscS* region in MJM2114 into pEVS79	**MJM3039**
MJM3042 =		Gib_ES114_rscS_DS_for	Gib_ES114_rscS_DS_rev	1.6 kb	Gibson assembly cloning of downstream *rscS* region in MJM2114 into pEVS79	
MJM2114 Δ*rscS*		ES114_US_ver	ES114_DS_ver	586 bp	Verification of Δ*rscS* by flanking the upstream/downstream junction	
		ES114_US_ver	DAT015F	520 bp	Verification of Δ*rscS*; no product due to one primer binding within *rscS*	
		Gib_ES114_syp_US_for	Gib_ES114_syp_US_rev	1.6 kb	Gibson assembly cloning of upstream *sypA* region in MJM1100 into pEVS79	**MJM3060**
MJM3062 =		Gib_ES114_syp_DS_for	Gib_ES114_syp_DS_rev	1.6 kb	Gibson assembly cloning of downstream *sypR* region in MJM1100 into pEVS79	
MJM1100 Δ*sypA-R*		Syp_ver_US_for	Syp_ver_DS_rev	503 bp	Verification of Δ*sypA-R* by flanking the upstream/downstream junction	
		Syp_ver_US_for	sypA_out	490 bp	Verification of Δ*sypA-R*; no product due to one primer binding within *sypA*	
		Gib_ES114_syp_US_for	Gib_ES114_syp_US_rev	1.6 kb	Gibson assembly cloning of upstream *sypA* region in MJM1117 into pEVS79	**MJM3066**
MJM3068 =		Gib_MB11B1_syp_DS_for	Gib_ES114_syp_DS_rev	1.6 kb	Gibson assembly cloning of downstream *sypR* region in MJM1117 into pEVS79	
MJM1117 Δ*sypA-R*		Syp_ver_US_for	Syp_ver_DS_rev	503 bp	Verification of Δ*sypA-R* by flanking the upstream/downstream junction	
		Syp_ver_US_for	sypA_out	490 bp	Verification of Δ*sypA-R*; no product due to one primer binding within *sypA*	
		Gib_SR5_syp_US_for	Gib_SR5_syp_US_rev	1.6 kb	Gibson assembly cloning of upstream *sypA* region in MJM1125 into pEVS79	**MJM3500**
MJM3501 =		Gib_SR5_syp_DS_for	Gib_SR5_syp_DS_rev	1.6 kb	Gibson assembly cloning of downstream *sypR* region in MJM1125 into pEVS79	
MJM1125 Δ*sypA-R*		SR5_syp_ver_for	SR5_syp_ver_rev	506 bp	Verification of Δ*sypA-R* by flanking the upstream/downstream junction	
		Gib_SR5_syp_US_for	sypA_out	1.9 kb	Verification of Δ*sypA-R*; no product due to one primer binding within *sypA*	
		Gib_MB11B1_syp_US_for	Gib_MB11B1_syp_US_rev	1.6 kb	Gibson assembly cloning of upstream *sypA* region in MJM1130 into pEVS79	**MJM3063**
MJM3065 =		Gib_MB11B1_syp_DS_for	Gib_ES114_syp_DS_rev	1.6 kb	Gibson assembly cloning of downstream *sypR* region in MJM1130 into pEVS79	
MJM1130 Δ*sypA-R*		Syp_ver_US_for	Syp_ver_DS_rev	503 bp	Verification of Δ*sypA-R* by flanking the upstream/downstream junction	
		Syp_ver_US_for	sypA_out	490 bp	Verification of Δ*sypA-R*; no product due to one primer binding within *sypA*	
		Gib_ES114_syp_US_for	Gib_ES114_syp_US_rev	1.6 kb	Gibson assembly cloning of upstream *sypA* region in MJM2114 into pEVS79	**MJM3069**
MJM3071 =		Gib_ES114_syp_DS_for	Gib_ES114_syp_DS_rev	1.6 kb	Gibson assembly cloning of downstream *sypR* region in MJM2114 into pEVS79	
MJM2114 Δ*sypA-R*		Syp_ver_US_for	Syp_ver_DS_rev	503 bp	Verification of Δ*sypA-R* by flanking the upstream/downstream junction	
		Syp_ver_US_for	sypA_out	490 bp	Verification of Δ*sypA-R*; no product due to one primer binding within *sypA*	
		Gib_ES114_binK_US_for	Gib_ES114_binK_US_rev	1.6 kb	Gibson assembly cloning of upstream *binK* region in MJM1130 into pEVS79	**MJM3082**
MJM3084 =		Gib_ES114_binK_DS_for	Gib_ES114_binK_DS_rev	1.6 kb	Gibson assembly cloning of downstream *binK* region in MJM1130 into pEVS79	
MJM1130 Δ*binK*		JFB_287_MB11B1	JFB_288	767 bp	Verification of Δ*binK* by flanking the upstream/downstream junction	
		JFB_287_MB11B1	JFB_365	624 bp	Verification of Δ*binK*; no product due to one primer binding within *binK*	
MJM3417 =		Gib_ES114_sypE_US_for	Gib_ES114_sypE_US_rev	1.6 kb	Gibson assembly cloning of upstream *sypE* region in MJM1100 into pEVS79	**MJM3416**
MJM1100 Δ*sypE* and		Gib_ES114_sypE_DS_for	Gib_ES114_sypE_DS_rev	1.6 kb	Gibson assembly cloning of downstream *sypE* region in MJM1100 into pEVS79	
MJM3423 =		syp4F	syp4R	780 bp	Verification of Δ*sypE* by flanking the upstream/downstream junction	
MJM3010 Δ*sypE*		syp5F	syp4R	772 bp	Verification of Δ*sypE*; no product due to one primer binding within *sypE*	
		Gib_MB11B1_sypE_US_for	Gib_MB11B1_sypE_US_rev	1.6 kb	Gibson assembly cloning of upstream *sypE* region in MJM1130 into pEVS79	**MJM3409**
MJM3410 =		Gib_MB11B1_sypE_DS_for	Gib_MB11B1_sypE_DS_rev	1.6 kb	Gibson assembly cloning of downstream *sypE* region in MJM1130 into pEVS79	
MJM1130 Δ*sypE*		for_ver_sypE	rev_ver_sypE	732 bp	Verification of Δ*sypE* by flanking the upstream/downstream junction	
		MB11B1_indel_for	MB11B1_indel_rev	779 bp	Verification of Δ*sypE*; no product due to both primers binding within *sypE*	
		Gib_ES114_sypE_N_for	Gib_ES114_sypE_N_rev	332 bp	Gibson assembly cloning of N-terminal *sypE* in MJM1100 into pEVS107	**MJM3340**
MJM3354 =		Gib_ES114_sypE_C_for	Gib_ES114_sypE_C_rev	1786 bp	Gibson assembly cloning of C-terminal *sypE* in MJM1100 into pEVS107	**and**
MJM1100 *sypE* (ntG33Δ)		Gib_pEVS79_ES_sypE_for	Gib_pEVS79_ES_sypE_rev	2118 bp	Gibson assembly cloning of *sypE* (ntG33Δ) into pEVS79	**MJM3352**
		ES114_indel_for	ES114_indel_rev	802 bp	Verification of *sypE* (ntG33Δ); stronger band with original allele.	
		Gib_MB11B1_sypE_N_for	Gib_MB11B1_sypE_N_rev	332 bp	Gibson assembly cloning of N-terminal *sypE* in MJM1130 into pEVS107	**MJM3338**
MJM3397 =		Gib_MB11B1_sypE_C_for	Gib_MB11B1_sypE_C_rev	1786 bp	Gibson assembly cloning of C-terminal *sypE* in MJM1130 into pEVS107	**and**
MJM1130 *sypE* (nt33::G)		Gib_pEVS79_MB_sypE_for	Gib_pEVS79_MB_sypE_rev	2118 bp	Gibson assembly cloning *sypE* (nt33::G) into pEVS79	**MJM3351**
		MB11B1_indel_for	MB11B1_indel_rev	779 bp	Verification of *sypE* (nt33::G); stronger band with corrected allele.	

>gBlock_erm
GGTCAGCCTCTAATGGCTCGTAAGATAGTGTAGGAAGCTTTATCGAACTGCGCGAAAGATCCCGAAGTTCCTATTCTCT
AGAAAGTATAGGAACTTCCTTAGAAGCAAACTTAAGAGTGTGTTGATAGTGCAGTATCTTAAAATTTTGTATAATAGGA
ATTGAAGTTAAATTAGATGCTAAAAATTTGTAATTAAGAAGGAGTGATTACATGAACAAAAATATAAAATATTCTCAAA
ACTTTTTAACGAGTGAAAAAGTACTCAACCAAATAATAAAACAATTGAATTTAAAAGAAACCGATACCGTTTACGAAAT
TGGAACAGGTAAAGGGCATTTAACGACGAAACTGGCTAAAATAAGTAAACAGGTAACGTCTATTGAATTAGACAGTCAT
CTATTCAACTTATCGTCAGAAAAATTAAAACTGAATACTCGTGTCACTTTAATTCACCAAGATATTCTACAGTTTCAAT
TCCCTAACAAACAGAGGTATAAAATTGTTGGGAGTATTCCTTACCATTTAAGCACACAAATTATTAAAAAAGTGGTTTT
TGAAAGCCATGCGTCTGACATCTATCTGATTGTTGAAGAAGGATTCTACAAGCGTACCTTGGATATTCACCGAACACTA
GGGTTGCTCTTGCACACTCAAGTCTCGATTCAGCAATTGCTTAAGCTGCCAGCGGAATGCTTTCATCCTAAACCAAAAG
TAAACAGTGTCTTAATAAAACTTACCCGCCATACCACAGATGTTCCAGATAAATATTGGAAGCTATATACGTACTTTGT
TTCAAAATGGGTCAATCGAGAATATCGTCAACTGTTTACTAAAAATCAGTTTCATCAAGCAATGAAACACGCCAAAGTA
AACAATTTAAGTACCGTTACTTATGAGCAAGTATTGTCTATTTTTAATAGTTATCTATTATTTAACGGGAGGAAATAAT
CTAGAATGCGAGAGTAGGGAACTGCCGAAGTTCCTATTCTCTAGAAAGTATAGGAACTTCAGCGCTCATGCACTTGATT
CCGGATCCCTAATTAGCGAACGCAGCTGGCTCTCCAA